Running title: Ontogenetic variation in G

Development of G: A test in an amphibious fish.

Joseph M. Styga[1,4*], Thomas M. Houslay[2,3], Alastair J. Wilson[3], and Ryan L. Earley[4]

1 Department of Biology, Culver-Stockton College, One College Hill, Canton, MO 63435, USA

2 Department of Zoology, University of Cambridge, Downing Street, Cambridge, CB2 3EJ, UK

3 Centre for Ecology and Conservation, University of Exeter-Penryn Campus, Cornwall, TR10 9FE, UK.

4 Department of Biological Sciences, University of Alabama, 300 Hackberry Lane, Box 870344, Tuscaloosa, AL 35487, USA

Word Count: 6,345

Author for Correspondence (*)
Joseph M. Styga
Culver-Stockton College
Science Center
One College Hill
Canton, MO 63435
Email: jstyga@culver.edu
Phone: (678) 641-3667

Abstract

Heritable variation in, and genetic correlations among, traits determine the response of multivariate phenotypes to natural selection. However, as traits develop over ontogeny, patterns of genetic (co)variation and integration captured by the **G** matrix may also change. Despite this, few studies have investigated how genetic parameters underpinning multivariate phenotypes change as animals pass through major life history stages. Here, using a self-fertilizing hermaphroditic fish species, mangrove rivulus (*Kryptolebias marmoratus*), we test the hypothesis that **G** changes from hatching through reproductive maturation. We also test Cheverud's conjecture by asking whether phenotypic patterns provide an acceptable surrogate for patterns of genetic (co)variation within and across ontogenetic stages. For a set of morphological traits linked to locomotor (jumping) performance, we find that the overall level of genetic integration (as measured by the mean-squared correlation across all traits) does not change significantly over ontogeny. However, we also find evidence that some trait-specific genetic variances and pairwise genetic correlations do change. Ontogenetic changes in **G** indicate the presence of genetic variance for developmental processes themselves, while also suggesting that any genetic constraints on morphological evolution may be age-dependent. Phenotypic correlations closely resembled genetic correlations at each stage in ontogeny. Thus, our results are consistent with the premise that – at least under common environment conditions - phenotypic correlations can be a good substitute for genetic correlations in studies of multivariate developmental evolution.

Keywords: **G**-matrix, genetic integration, ontogeny, *Kryptolebias*

Introduction:

Integration, a characteristic of the multivariate phenotype, describes patterns of correlation among functional traits (Pigliucci, 2003, Perez-Barrales et al., 2014, Margres et al., 2015). While most often studied at the phenotypic level (Klingenberg and Marugan-Lobon, 2013), if the goal is to understand multivariate evolution then studies of genetic integration are particularly informative (Klingenberg, 2014). This is because the degree to which any trait can evolve under selection ultimately depends not only on the extent to which it varies due to genetic factors (referred to as 'genetic variance'), but also on the genetic correlations it shares with other traits (Lande, 1979, Lande, 1980, Lande and Arnold, 1983, Arnold, 1992, Arnold et al., 2008, Björklund et al., 2013). These patterns of genetic (co)variation within and between traits can be represented as the genetic variance/covariance matrix (**G**). While phenotypic integration is itself expected to arise from past selection favoring particular trait combinations, the structure of **G** also has the potential to facilitate or constrain adaptive evolutionary responses to current selection (Porto et al., 2009, Walsh and Blows, 2009). This is because genetic correlations among traits will prevent any one trait from evolving independently of others, even if this would in principle be advantageous (Cheverud, 1996, Armbruster et al., 2014).

In recent years, it has become increasingly evident that genetic variances and correlations do not remain static as organisms develop and age (Badyaev and Martin, 2000, Blumstein et al., 2013, Class and Brommer, 2015). Genetic variances associated with life history (Charmantier et al., 2006) and morphological traits (Björklund, 1997, Badyaev and Martin, 2000) often vary across ontogeny. For specific trait pairs, it is also known that genetic correlations can change with age or life stage (Moran, 1994, Watkins, 2001, Aguirre et al., 2014). However, few studies have examined changes in a more fully multivariate context, comparing **G** among larger sets of

92 traits to test for shifting patterns of genetic integration across development (Cheverud et al.,
93 1983, Aguirre et al., 2014). Because selection acts on multivariate phenotypes (Ellis et al., 2014),
94 and potentially in different ways over the full timeline of development (Gignac and Santana,
95 2016), scrutinizing changes in **G** across ontogeny may help us better understand not only past
96 evolutionary processes but also the potential for future adaptive evolution. The latter point
97 follows because age-specific **G** matrices can be used to evaluate the potential for genetic
98 constraint in relation to selection acting on phenotypic state at that age. However, it is also true
99 that changes in **G** across age represent a (multivariate) genotype-by-age interaction (GxA),
100 which can equally be conceptualized as genetic variance for the developmental trajectory (just as
101 GxE is genetic variance for plasticity; e.g., Wilson et al., 2008, Roff and Wilson, 2014 for
102 didactic explanations of this equivalence). Thus, to the extent that current selection acts directly
103 on development as a process (rather than on age-specific phenotypic state), the presence of GxA
104 is required for further evolution of the developmental trajectory.
105 While valuable, wider estimation of age-specific **G** matrices for traits known (or
106 hypothesized) to contribute to functional integration is logistically challenging. Data
107 requirements are high and further logistic constraints can arise from the characteristics being
108 studied (Damián et al. 2017). For sexual diploid organisms, it is also generally necessary to
109 utilize large breeding designs, or recover pedigree information using molecular data. When **G**
110 cannot readily be estimated then **P**, the phenotypic variance-covariance matrix, has been used in
111 its place (Marroig and Cheverud, 2001, Steppan et al., 2002). This strategy has become
112 especially commonplace in studies related to morphological integration (Eroukhmanoff and
113 Svensson, 2008). The primary criticism of such an approach is that, because **P** combines both
114 genetic (**G**) and environmental (**E**) components of (co)variance, its reliability as a substitute for

115 **G** cannot be assured (Arnold, 1981, Lofsvold, 1986, Kruuk et al., 2008). Despite this, **P** has been
116 shown to be a reliable predictor of **G** on many occasions (Atchley et al., 1981, Cheverud, 1995,
117 Arnold and Phillips, 1999) and has given rise to Cheverud's conjecture (Cheverud, 1988), which
118 states that phenotypic correlations can be used as a substitute for genetic correlations. However,
119 both **G** and **E** could change independently of one another across development, such that changes
120 in **P** may not reflect changes in **G** (Badyaev and Martin, 2000, Mitteroecker and Bookstein,
121 2009). Because of this, **P** may be an appropriate substitute for **G** only at certain stages of
122 ontogeny. Few studies (Cheverud et al., 1983, Leamy and Cheverud, 1984, Badyaev and Martin
123 2000), however, have looked at whether the relationship between **P** and **G** is stable over
124 development.
125 Mangrove rivulus fish, *Kryptolebias marmoratus*, are an excellent vertebrate model in
126 which to test for ontogenetic changes in **G** using a quantitative genetic framework. Individuals
127 exist as self-fertilizing hermaphrodites (Earley et al., 2012), a unique breeding strategy among
128 vertebrates that allows for the production of many replicates of a single genotype without the
129 need for complex breeding designs. We focus here on a set of morphological characters that we
130 have previously shown are associated with a fitness-related functional performance characteristic
131 – terrestrial jumping - using animals that were not involved in the present study (Styga et al.,
132 2018). Terrestrial jumping is an important behavior in mangrove rivulus fish, as it allows
133 individuals to effectively traverse land to locate new pools of water or patches of damp leaf litter
134 during periods of low tide (Magellan, 2016). A jump is produced when an individual flexes its
135 axial muscles, places its body weight on its caudal peduncle (i.e. the area directly adjacent to its
136 caudal fin), and launches itself from the ground (Gibb et al., 2011, Ashley-Ross et al., 2014). The
137 fitness advantage associated with high terrestrial jumping may be most apparent in the field,

where other less terrestrially adept fish species (e.g., *Gambusia*) have been found dead in dried pools, while *K. marmoratus* has been found living on land just outside of these pools (Taylor, 2012). Because of the association between skeletal morphology and jumping performance, positive selection on jumping has been postulated to drive corresponding changes in morphology (Gibb et al., 2013).

We have previously found that jumping performance is significantly correlated with bone dimensions within the caudal peduncle, the posterior portion of the body of a fish (Styga et al. 2018). Jumping is positively correlated with lengths of the epural (EPL) and hypural (HYPL), and negatively correlated with the angle of the epural (EPA) relative to the vertebral centrum (Fig. S1). However, these phenotypic relationships were only present in young (<120 days post hatching, DPH) fish (see Fig. 2 in Styga et al. 2018), and not in mature (250-500 DPH) or old (>500 DPH) fish, possibly reflecting a decreased reliance on these bones for jumping at later ages (Styga et al. 2018). Therefore, in the present study, we focus on studying ontogenetic variation in the genetic (co)variance structure among these morphological traits at various points from hatching to sexual maturity (0-120 DPH range) (Cole and Noakes, 1997). In what follows, we characterize (co)variation at both phenotypic (**P**) and genetic (**G**) levels for six skeletal characteristics (Fig. S1), and standard length (SL), at three developmental stages (1, 15, and 100 DPH). In mangrove rivulus, the skeletal morphology of the caudal peduncle is not perfectly bilaterally symmetrical (Styga et al., 2018); therefore, we assessed phenotypic and genetic (co)variation for traits on opposing sides of the vertebral column (i.e. EPL and PHPL and EPA and PHPA). We determine integration among these traits at both phenotypic and genetic levels, and also test Cheverud's conjecture (Cheverud, 1988) that phenotypic correlations can be used to reliably estimate genetic correlations at each age. We formally test the hypotheses that: (i)

phenotypic (co)variance (**P**) among traits will vary among age classes, (ii) traits are genetically variable, (iii) trait genetic variance will be age-dependent, (iv) the full genetic (co)variance (or correlation) structure **G** will change between ages, and (v) **P** provides a valid proxy of **G** matrix at each stage in development.

Methods:

Animal Care and Specimen Collection

Specimens (n=1,066) that were used in this study were obtained from (F2-F12) progenitors acquired from 44 genotypes; however, most specimens were obtained from F2 or F3 progenitor stocks (Table S1). Because the vast majority of animals (91%) came from F2 or F3 progenitor stocks, we did not include 'generation' in our models. All experimental fish were produced by selfing of genetically distinct progenitors with each progenitor having a unique genotype. We utilized 44 isogenic or near-isogenic lineages from our progenitor stock. Microsatellites were used to identify distinct multilocus genotypes (i.e. unique combinations of alleles present across 32 loci), with isogenic lineages being derived from wild-caught progenitors that were homozygous at all 32 loci, and near-isogenic lineages being derived from wild-caught progenitors that were homozygous at, on average, 28 loci (range: 16-31, median: 30) (Mackiewicz et al. 2006; Tatarenkov et al., 2011). *K. marmoratus* is an androdioecous species, meaning that only male or hermaphroditic individuals make up the population (Turner et al., 1992). In our study, we focused on morphological variation in hermaphrodites. As a result, we excluded any males from our study, which are easily recognizable by the presence of orange pigmentation on the body and a faded (or absent) eyespot on the dorsal portion of the caudal peduncle (Scarsella et al., 2018).

Progenitors, their eggs, and hatchlings were housed under common garden conditions (12 hour light: 12 hour dark photoperiod cycle, at 26°C, and in 25 ppt saltwater). Progenitors were fed 4 mL brine shrimp nauplii (*Artemia* spp.) while hatchlings were fed 1 mL brine shrimp nauplii on a daily basis. Both progenitors and hatchlings were housed individually for the duration of the experiment. Each progenitor was housed in 750 mL Rubbermaid® TakeAlong® Deep Square containers with spawning substrate (i.e. Poly-Fil®), which was checked for eggs weekly. Once obtained from the spawning substrate, eggs were transferred to 59 mL, clear polystyrene cups until hatching. Complete water changes were conducted on each egg cup weekly to refresh the water. The date on which eggs were laid was also recorded. At the time of hatching, each individual larval fish was transferred to one 473 mL plastic cup filled 75% with 25 ppt water. Hatchlings were kept in these enclosures until they reached a predetermined age. Hatching date was recorded for all individuals. We included time spent in the egg (interval [days] between date laid and hatching date; hereafter referred to as 'Time') as a covariate in our models (see below) to account for phenotypic variance due to differences in developmental time within the egg. All fish husbandry was done in accordance with the University of Alabama's Institutional Animal Care and Use Committee (Protocol #: 14-05-0070). A total of 10-15 individuals were collected from most genotype-age combinations (1, 15, and 100 days post hatching [DPH]) (Table S1). Although our sampling for each genotype-age combination was not completely balanced (Table S1), other studies have found that unbalanced designs in quantitative genetic studies do not mandate restrictive assumptions about variance/covariance structures (Fry, 1992). We limited our focus to the first 100 DPH because this is the age, on average, at which *K. marmoratus* typically reaches sexual maturity (Cole and Noakes, 1997), and because jumping performance is only significantly correlated with caudal peduncle bone morphology before this

age (Styga et al., 2018). Each individual was euthanized in a lethal dose of pharmaceutical grade MS-222 (Finquel®), which was buffered to a neutral pH with sodium bicarbonate. Each hatchling was then stored individually in a 1.5 mL centrifuge tubes filled with 100% ethanol prior to morphometric analysis.

Bone Morphometrics

Specimens were cleared and stained individually in 1.5 mL centrifuge tubes, using a modified version of the procedure developed by Webb and Byrd (1994) (Table S2). The clearing and staining process produces transparent specimens with bones stained deep red, which we then photographed alongside a metric ruler in standard ichthyological position under a Zeiss 2000-C stereoscope using a Canon® Powershot G9 (Fig. S1). Images were then scaled to the nearest mm in ImageJ software (Schneider et al., 2012). Within ImageJ, we measured standard length (SL) of the specimen, length and angle of epural (EPL and EPA) and parahypural bones (PHPL and PHPA), and length and width of hypurals (HYPL and HYPW) (7 measurements; Fig. S1) from each fish. Although ossification is often not complete at the beginning of larval development in fishes (Mabee et al., 2000), in our study, all individuals were fully ossified at 1 DPH (Fig. S2). Therefore, we did not have to consider variance in the presence/absence of bones across ages when estimating **G**.

Statistical analysis

We analyzed data using used both univariate and multivariate linear mixed effect models to test our various hypotheses (described in detail below). Models were fitted with ASreml-R 3.0

229 (Butler, 2009, Gilmour et al., 2002) in R version 3.4.1 (R Core Team, 2017). All trait values
230 were converted to standard deviation units (SDU) using the observed SD across all ages. This
231 facilitates multivariate model fitting by removing among-trait scaling differences while retaining
232 any among-age differences in (co)variance structures. Except where explicitly stated otherwise,
233 all results are presented on this scale. In some instances, results are also presented in within-age
234 class standard deviations such that, for example, age-specific genetic variances can be interpreted
235 analogously to age-specific heritabilities. In addition to bone measurements, we treat standard
236 length (SL) as a morphological trait in its own right that may be genetically correlated with other
237 traits. Any such correlations with SL might shape evolutionary change in other aspects of
238 morphology (Marroig et al., 2005) so we modeled this as an additional response variable rather
239 than a 'nuisance' covariate.
240 To estimate genetic parameters, we included a random effect of genotype. Because
241 experimental fish were produced by selfing of genetically distinct progenitors, this analysis
242 partitions "among genotype" from total variance analogous to a study using recombinant inbred
243 lines (as opposed to a family-based analysis of an outcrossing diploid). Statistical inferences
244 were based on comparing nested models using likelihood ratio tests (LRTs) and on generating
245 approximated 95% confidence intervals (see below). For LRTs we estimated χ^2_n as twice the
246 difference in model log likelihoods. The number of degrees of freedom (n) was conservatively
247 set to the number of additional parameters in the more complex model except when testing a
248 single variance component in which case we assumed the test statistic to be asymptotically
249 distributed as an equal mix of χ^2_0 and χ^2_1 (written below as $\chi^2_{0,1}$; Visscher, 2006). In each model
250 we controlled statistically for any effect of 'Time', defined as the differences in number of days
251 between when an individual egg was laid and when it hatched, by including it as a fixed effect on

all response variables. Although not directly relevant to the biological hypotheses being tested and so not discussed further below, statistical inferences on Time are presented in Table S3 for completeness.

Phenotypic (co)variance within and across ages

We estimated age-specific phenotypic variance-covariance matrices ($\mathbf{P}_1$, $\mathbf{P}_{15}$, $\mathbf{P}_{100}$) using a separate multivariate (7 trait) model for each age. These models had no random effects, such that all phenotypic (co)variance (conditional on 'Time') is allocated to the residual component. Using the matrix estimates and the sampling covariances of each element with them, we applied a parametric bootstrap approach (as described in Boulton et al., 2015) with 5,000 draws to generate approximate 95% confidence intervals for each element (and, for covariance terms, the corresponding correlation) of $\mathbf{P}_1$, $\mathbf{P}_{15}$, and $\mathbf{P}_{100}$. Confidence intervals are approximate since the bootstrap approach makes an assumption of multivariate normality that may well be violated (see Boulton et al., 2015, Houle and Meyer, 2015). Consequently, we do not calculate p-values but conclude (nominal) statistical significance when 95% confidence intervals do not include zero. We used bootstrap samples to test for significant differences between three aspects of age-specific **P** matrices: total phenotypic integration, as calculated by the mean squared correlation among all traits; total phenotypic variation, as calculated by the matrix 'trace' (i.e. sum of diagonal elements); and pairwise-trait phenotypic correlations (rP) (see Houslay et al., 2017). For each pair of ages we also calculate the elements of the 'difference matrices' (e.g. $\mathbf{P}_1 - \mathbf{P}_{15}$) and use the bootstrapped samples to generate 95% confidence intervals for each element (i.e. pairwise difference between age groups in a variance or covariance estimate). We do this because, while non-overlapping 95% confidence intervals on age-specific elements of **P** denote

(nominally) significant differences at $\alpha = 0.05$, it does not always follow that the difference in effect size is non-significant when 95% intervals do overlap (Austin et al. 2002).

Genetic variation and GxA for each trait

To determine whether individual traits harbored significant genetic variance across ontogeny, and whether there was a genotype-by-age interaction (GxA), we fitted a series of three nested trivariate models using age-specific observations as the three response variables (e.g., SL age 1, SL age 15, SL age 100). Each model included a fixed effect of 'Time' on each response and a heterogeneous residual structure allowing non-genetic (i.e., residual) variance to differ among age-classes. Model A contained no genetic effects, Model B allowed genetic variance but assumed a single genetic parameter and an absence of GxA (such that, for any pair of ages x,y, $V_{Ax} = V_{Ay}$ and $r_{Gx,y} = +1$), while Model C estimated a fully unstructured matrix (i.e., genetic variance for each age and covariance between ages). LRT comparison of A and B provides a test for genetic variance, while comparison of B and C tests for GxA.

Genetic integration of morphological traits

We then used multivariate (7 trait) models to estimate the age-specific genetic variance-covariance matrices ($\mathbf{G}_1$, $\mathbf{G}_{15}$, $\mathbf{G}_{100}$) among morphological traits and test for changes across ontogeny (in a similar manner to our analyses of $\mathbf{P}_1$, $\mathbf{P}_{15}$, $\mathbf{P}_{100}$). For each age-specific model we included a fixed effect of 'Time' and a random effect of genotype on each trait. The non-genetic (residual) structure was modelled as an unstructured matrix, as was **G.** However, for comparison we also fitted a simpler model in which we used diagonal matrix (i.e., genetic variances only, all among-trait covariances assumed to be zero). LRT comparison of full and simplified (i.e.,

298 diagonal **G** only) provided a test of whether significant genetic covariance exists across all traits
299 at the age in question. Although the data were scaled to overall (i.e., across all age classes)
300 standard deviations as described earlier, we also estimated age-specific **G** matrices with data
301 scaled to within-age SDUs. This scaling does not affect correlation structure but means that the
302 diagonal elements can be interpreted as analogous to heritabilities (i.e. the proportion of variance
303 – at that age – that is attributable to genetic effects). Comparisons among age classes then
304 employed the bootstrapping procedure described earlier to compare the total genetic variation
305 (i.e. trace, on both scales) across ages, pairwise-trait correlations (r) between each age group (see
306 Houslay et al., 2017), and the level of genetic integration (calculated as the mean squared
307 correlation across all traits).
308 Finally, as a test of Cheverud's conjecture, we used our bootstrapped samples for **P** and
309 **G** at each distinct age group (e.g., $\mathbf{P}_1$ vs $\mathbf{G}_1$) to test whether these matrices differ significantly in
310 estimated correlation structure among morphological traits.
311
312 **Results:**
313 *Phenotypic (co)variance within and across ages*
314 Confidence intervals estimated from our bootstrapping procedure revealed that the sum of
315 phenotypic variance for all traits (i.e. trace) was significantly higher at $\mathbf{P}_{100}$ than at $\mathbf{P}_1$ and $\mathbf{P}_{15}$,
316 while multivariate phenotypic variance did not differ significantly between $\mathbf{P}_1$ and $\mathbf{P}_{15}$ (Fig. 1;
317 Table S4). Interestingly, different trait types contributed in opposing ways to the changes (and/or
318 lack thereof) in **P** matrix trace with age. Specifically, while phenotypic variance in all linear
319 distance measurements (EPL, PHPL, HYPL, HYPW, and SL) increased with ontogeny, the
320 opposite pattern was seen for the angular measurements (EPA and PHPA) (Table 1). For each of

the 7 traits, we found significant differences in phenotypic variance between $\mathbf{P}_1$ and $\mathbf{P}_{15}$, $\mathbf{P}_1$ and $\mathbf{P}_{100}$, and $\mathbf{P}_{15}$ and $\mathbf{P}_{100}$ (Table 2).

As estimated by the mean-squared correlation, the extent of phenotypic integration (i.e. the relative strength of correlations among traits) differed among ages (point estimates of mean-squared correlation were 0.22, 0.25 and 0.17 at ages 1,15 and 100 respectively). Based on bootstrapped confidence intervals, both $\mathbf{P}_1$ and $\mathbf{P}_{15}$ were significantly more integrated than $\mathbf{P}_{100}$ (Fig. 1; Table S4) but $\mathbf{P}_1$ and $\mathbf{P}_{15}$ were not significantly different (Fig. 1; Table S4). Consideration of each off-diagonal element of **P** also revealed numerous differences between ages in the pairwise relationships among traits (Fig. 2 and 3; Tables S5 and S6). Scaled to correlations (which are perhaps easier to interpret than covariance), we find that 16 of the 21 pairwise-trait associations differed significantly between $\mathbf{P}_1$ and $\mathbf{P}_{15}$, 10 between $\mathbf{P}_1$ and $\mathbf{P}_{100}$, and 9 between $\mathbf{P}_{15}$ and $\mathbf{P}_{100}$ (Fig. 3; Table S6). Nonetheless, despite significant changes in correlation magnitude, it is also the case that many relationships were at least qualitatively consistent across ontogeny. For instance, in each age group: i.) EPL was significantly positively related to PHPL, HYPL, HYPW, and SL, ii.) PHPL was significantly positively related to HYPL, HYPW, and SL; iii.) HYPL was significantly positively related to HYPW and SL; and iv.) HYPW was significantly positively related to SL (Fig. 2; Table S5). On the contrary, only one (i.e. the correlation between PHPA and EPA) of the significant negative correlations evident within $\mathbf{P}_1$ (many of which involved PHPA) was maintained throughout ontogeny.

Genetic variation and GxA for each trait

Based on the set of trivariate models formulated for each phenotypic trait, LRT comparisons showed that each trait exhibited significant genetic variance across ontogeny (see 'Genetic

Variance' in Table 3). In addition, the unstructured genetic (co)variance model provided a better fit to our data than the model that included a single genetic parameter. Thus, for each trait we find evidence of a significant genotype-by-age interaction (GxA) (Table 3). Significant GxA for each trait means that each trait has age-specific genetic variance, which will be reflected as between-age genetic correlations of less than +1 and/or changes in genetic variance with age. Here, for most traits, between-age genetic correlations were significantly positive between 1 and 15 DPH and 1 and 100 DPH, and significantly negative between 15 and 100 DPH (Table 3). Genetic variance estimates from these models also differed across ages. They are not presented here but were very similar to the corresponding estimates obtained from multi-trait models fitted to each age class (presented and discussed below).

Genetic integration of morphological traits within each age

Multivariate (7 trait) models fitted to each age group, revealed significant among-trait genetic covariance structure contributing to morphological integration (Fig. 2; Table S7). In all three age classes, a model that included genetic covariances among traits was significantly better than the model that assumed a diagonal **G** matrix only (χ^2_{21}=188, P=<0.001; χ^2_{21}=207, P=<0.001; χ^2_{21}=176, P=<0.001 at ages 1,15 and 100 respectively). Confidence intervals estimated from our bootstrapping procedure revealed that total genetic variance for the multivariate phenotype (i.e. trace of **G**) was significantly lower at $\mathbf{G}_{15}$ and $\mathbf{G}_{1}$ than at $\mathbf{G}_{100}$ (Fig. 1; Table S4). The trace of $\mathbf{G}_{1}$ did not differ significantly from that of $\mathbf{G}_{15}$. For individual traits, nominally significant differences in genetic variance were found in 11 out of 21 possible between-age comparisons (Table 2). One trait (SL) had a significant change in genetic variance between 1 and 15 DPH, and five traits changed significantly between 15 and 100 DPH, and 1 and 100, respectively.

These significant effects were driven by a clear pattern of increasing genetic variance with age for the linear distance traits (but not for the angular measurements EPA and PHPA). Note, however, that no such pattern is evident when expressing (total) genetic variance as a proportion of (total) phenotypic variance within each age class (i.e. on a 'heritability' scale). On this scale, there were no significant differences between ages in **G** matrix traces (Fig. 1; Table S4) or in trait-specific 'heritabilities' (Table 2).

Using mean squared-genetic correlation to estimate age-specific genetic integration we found a qualitative pattern of decreasing integration with increased age, but we note that comparisons of this metric across age-specific **G** matrices were not statistically significant (Fig. 1; Table S4). Despite the lack of significant change in overall genetic integration, there were some differences in pairwise genetic correlations between age groups that were significant at the nominal level (Fig. 2 and 3; Table S7 and S8). Specifically, of the 21 pairwise genetic correlations in **G**, 5 estimates differed significantly between $\mathbf{G}_1$ and $\mathbf{G}_{15}$, 5 between $\mathbf{G}_1$ and $\mathbf{G}_{100}$, but none between $\mathbf{G}_{15}$ and $\mathbf{G}_{100}$ (Fig. 3; Table S8). Although this provides evidence for changes in genetic correlation structure, we acknowledge the possibility of Type I error here and also note that, as in **P,** most between-trait associations in **G** were qualitatively maintained across ontogeny. For instance, in each age group: i.) EPL showed a positive genetic correlation with PHPL, HYPL, HYPW, and SL; ii.) PHPL showed a positive genetic correlation with HYPL, HYPW, and SL; iii.) HYPL showed a positive genetic correlation with HYPW, and SL; and iv.) HYPW showed a positive genetic correlation with SL.

Similarity of correlations in **P** *and* **G** *within each age*

389 At each age, we found support for Cheverud's conjecture – pairwise correlations in **P** did an
390 excellent job of predicting correlations in **G (**Table S9). Of the 21 pairwise trait correlations at
391 each age, only 4 differed significantly between $\mathbf{P_1}$ and $\mathbf{G_1}$, 2 between $\mathbf{P_{15}}$ and $\mathbf{G_{15}}$, and 2 between
392 $\mathbf{P_{100}}$ and $\mathbf{G_{100}}$. In seven of these 8 instances, genetic and phenotypic correlation estimates were
393 consistent in sign. The mean (SE) difference in magnitude between phenotypic and genetic
394 correlations was -0.04 (0.04) at age 1, -0.1 (0.02) at age 15 and -0.09 (0.01) at age 100.
395
396 **Discussion**
397 Our results provide evidence in support of all five hypotheses advanced. First, for the set
398 of morphological traits examined, we found that the among-trait phenotypic variance-
399 covariance-correlation structure **P** differed between ages (Fig. 2; Table S5). In particular, the
400 variance of traits measured as linear distances increases with age (Table 1). For a given size-
401 related trait, differences in development (i.e. growth) must cause increased variance in size with
402 age (Chevin, 2015). Thus, the pattern detected here means that there is variation in the
403 multivariate developmental trajectory. Notably however, this not only impacts variances, but also
404 leads to an overall decline in phenotypic integration with age. Second, we show that phenotypic
405 variance is underpinned by genetic variation for all traits at all ages (Table 3). Third, for each
406 trait considered individually there is evidence of genotype-by-age interaction (GxA) and
407 fluctuations in genetic correlations between ages (Table 3). Thus, there appears to be genetic
408 variance in developmental trajectory. Fourth, at the multivariate level, GxA is reflected by
409 changes in **G** across ages (Fig. 2; Table 3). In particular, there is an increase in overall
410 (multivariate) genetic variance with age (Fig. 1; Table S4), which mirrors the phenotypic pattern
411 (Fig. 1; Table S4). Genetic integration among the traits also appears to decline with age (Fig. 1;

412 Table S4), although we acknowledge that this effect is not statistically significant. Finally, we
413 also find support for our fifth hypothesis - that **P** is a valid proxy for **G** – in terms of
414 understanding the among-trait correlation structure at each developmental stage (Table S9). In
415 general, phenotypic correlations should more closely approximate genetic correlations as genetic
416 variance underlying traits increases (Lande, 1982, Hadfield et al., 2007, Delahaie et al., 2017).
417 Thus, because genetic variance was relatively high for most of our traits at all ages considered,
418 the similarity between age-specific **G** and **P** matrices is perhaps not surprising. We also note that
419 all fish were raised under standardized lab conditions such that environmental sources of trait
420 (co)variation were both limited and common to all genotypes.
421
422 **Genetic effects and constraints on future evolution**
423 Morphological traits, and the relationships between them, are influenced heavily by
424 genetic factors at each stage in ontogeny. We found that genetic variance across all traits was
425 significantly lower at 1 and 15 compared to 100 DPH (Fig. 1). The increase in overall
426 (multivariate) genetic variance with age might initially suggest that selection on caudal peduncle
427 morphology should be more effective at driving evolutionary change in older fish. However, the
428 non-genetic component of variance also increases such that the relative contribution of genetic
429 factors to phenotypic variance is actually relatively stable. Indeed, when traits were scaled to
430 standard deviation units calculated within each age group (i.e. the 'heritability' scale), we found
431 that for most traits (not including EPA and PHPA), genetic variance was large, explaining > 40%
432 of the phenotypic variance within each age group.
433 The maintenance of high genetic variance for most traits across ontogeny may be related
434 to high spatial heterogeneity within the mangrove ecosystem. Noting that our lab population was

435 founded from multiple field collection sites, spatial heterogeneity (within and among field sites)
436 may have selected different genotypes (i.e., isogenic lineages) – with different phenotypes - to
437 occupy specific habitats (Pantel et al., 2011). This scenario, which is often referred to as the
438 'frozen niche model', can maintain standing levels of genetic variance in asexual (or, in our case,
439 selfing) species similar to those found in sexual species (Jokela et al., 1997, Negovetic and
440 Jokela, 2001, Niklasson et al., 2004).
441 Genetic relationships between traits were largely stable in sign over ontogeny, although
442 some changes in genetic correlations (notably in magnitude) with age were found. In general,
443 covariance in **G** influences multivariate evolutionary trajectories by imposing constraints on the
444 response to selection (Badyaev and Martin, 2010, Huchard et al., 2014, Nilsson-Örtman et al.,
445 2015). In the simplest case of two traits, a genetic correlation may prevent traits from becoming
446 independently optimized by selection, resulting in a potential trade-off. In this study, the positive
447 correlation between HYPL and EPA at 1 DPH may represent one of these trade-offs. HYPL is
448 positively, and EPA is negatively, related to jumping performance in young fish (i.e. <120 DPH)
449 (Styga et al., 2018). Although the functional link between these bones and jumping may not be
450 relevant to 1 DPH individuals because they do not jump, it may be important for other
451 performance characteristics used by 1 DPH individuals such as the aquatic C-start, which
452 utilizes similar motor patterns as the tail-flip jump (Perlman and Ashley-Ross 2016). Although
453 the same relationship was also found at 100 DPH it may not represent a trade-off here because
454 there appears to be decreased reliance on these bones as key determinants of jumping
455 performance at this age (Styga et al., 2018). Indeed, at adulthood, other characteristics (i.e.
456 strong muscles and well-developed neuromuscular junctions) may be playing a greater role in
457 influencing jumping performance.

458 Taking a more fully multivariate view, despite the relatively high levels of genetic
459 variance overall (at each age), if there are directions in multivariate trait space characterized by
460 low genetic variance, then adaptive evolution in this direction is – at least relatively - constrained
461 (Schluter, 1996; Björklund and Gustafsson, 2013). In fact, though the pattern was not significant,
462 comparison of **G** matrices among ages suggests higher genetic integration in the youngest fish.
463 This actually implies greater constraint here, at least in the limited sense that traits comprising
464 the multivariate phenotype are less able to evolve independently at, for example, 1 DPH vs 100
465 DPH. It is difficult to say more precisely what this means for expected evolution of the caudal
466 peduncle since we currently lack quantitative estimates for age-specific selection gradients on
467 morphological phenotype. An alternative view of the same phenomenon – namely multivariate
468 GxA – arises if we consider the developmental process (rather than age-specific state) as the
469 'target' of selection. GxA means there is genetic variance in, and so evolutionary potential of, the
470 ontogenetic trajectory of (multivariate) morphology. In this study, (genetically) distinct
471 developmental trajectories increase the observed (genetic) variation in morphology over 100
472 days of development.
473
474 **Does the G matrix reflect past selection?**
475 **G** (and **P**) might reflect historical selection favoring particular trait combinations at
476 different ages (Herrel and Gibb, 2006, Gignac and Santana, 2016, Penna et al., 2017). For
477 example, strong correlations among bones and muscles in young jackrabbits and guinea pigs
478 appear to result from strong selection for hopping and running performance, respectively, in this
479 age group (Carrier, 1983, Trillmich et al., 2003). However, ontogenetic variation in covariance
480 structure may reflect historical age-dependent correlational selection on interactions among

multiple traits so long as those interactions (at one time) improved fitness (Armbruster et al. 2014). Alternatively, directional selection on multiple traits simultaneously may have contributed to age-dependent genetic covariance (Penna et al., 2017). Either way, we expect that if historical selection on performance has been strong, then there should be strong correlations between traits in the direction that would have increased performance. In the case of the skeletal morphology within the caudal peduncle and its relationship to jumping performance, this means that **G** should depict a strong negative correlation between EPA and EPL/HYPL, and strong positive correlation between HYPL and EPL (Styga et al., 2018).

In this study, we found that the genetic correlations at 15 and 100 DPH are largely consistent with strong historical selection on jumping performance, although there were a few caveats (i.e. some of the correlations between traits in the direction that would increase jumping performance were not significant). We also found that genetic correlations at 1 DPH were not consistent with strong historical selection on jumping performance at this age (i.e. there was a significant positive relationship between HYPL and EPA). This result should, however, be considered in the context that 1 DPH individuals do not jump (Ashely-Ross pers. comm.).

The known functional relationship between caudal peduncle morphology and terrestrial locomotion performance (Styga et al., 2018) does not preclude other relationships that may complicate our interpretation. For instance, burst swimming facilitates predator avoidance in many fish larvae (Hale, 1999), and might hypothetically require a totally different morphological architecture (Gibb et al., 2013). Equally, relationships among bone dimensions could change adaptively with age to maintain locomotor performance in the face of other development change not considered here (e.g., change in mass, gonad or digestive morphology) (Badyaev and Martin, 2000). It is also possible that phenotypic integration is only critical for jumping performance

early on (i.e. 15 DPH) because other mechanisms (e.g. motor learning) are able to compensate later. It seems clear that the complex relationships between natural selection, form and function, and genetic covariance structure across ontogeny require further investigation.

Our study investigated ontogenetic variation in genetic (co)variance, while maximally controlling for any environmental variation, in a vertebrate species that exhibits a unique reproductive system where self-fertilization predominates. Because offspring were derived from isogenic lines, the **G** estimated from this study should be viewed as a broad-sense genetic variance-covariance matrix instead of an additive genetic variance-covariance matrix common in other quantitative genetic studies (Careau et al., 2015). As such, while **G** does a good job of predicting **P** at each stage in ontogeny, we should be wary of generalizing without considerable scrutiny to outbred sexual diploids and to situations where individuals are likely to vary due to exposure to environmental factors, unless those factors can be identified and controlled/modelled.

Summary

In our study, we have demonstrated that genetic (co)variance structures among performance-related morphological traits are age dependent. This multivariate GxA can be conceptualized in two alternative ways: as shifting patterns of evolutionary constraint for responses to selection on age-specific morphology; or as the presence of genetic variance in the multivariate developmental trajectory itself. Regardless of whether the primary interest is in predicting future evolution or in understanding historical processes, it is important to bear in mind that adaptive phenotypes are produced by selection acting on heritable variation present throughout the full scope of development (Kingsolver and Pfenning, 2014). Consequently,

appreciating whether, and to what extent, **G** matrices change across ontogeny is an important - albeit empirically challenging – task. In this regard, we note that support for our final hypothesis is encouraging in a pragmatic sense. Specifically, in accordance with Cheverud's conjecture, phenotypic correlations did an excellent job at predicting genetic correlations at each stage in development. While using **P** as a proxy for **G** always entails assumptions, our results suggest age-specific phenotypic patterns provide useful information for understanding the evolution of integration and development of multivariate morphology.

ACKNOWLEDGEMENTS

We would like to thank Andrew Burks, Brent Ishii, Calli Perkins, Abigail Sisti, Mark Smith, and Courtney Zacharias for helping with data collection. We would also like to thank Jane Rasco for her help with clearing and staining fish specimens. All animal care was done in accordance with The University of Alabama's Institutional Animal Care and Use Committee (IACUC) (Protocol #:14-05-0070).

CONFLICT OF INTEREST

The authors declare no conflict of interest.

DATA ARCHIVING

The data used in this manuscript has been achieved in Dryad repository: doi:10.5061/dryad.m56pj5b.

560
561 **References:**

562 Aguirre JD, Blows MW, Marshall DJ (2014). The genetic covariance between life cycle stages
563 separated by metamorphosis. *Proceedings of the Royal Society B* **281**:20141091.

564 Armbruster WS, Pelabon C, Bolstad GH, Hansen TF (2014). Integrated phenotypes:
565 understanding trait covariation in plants and animals. *Philosophical Transactions of the*
566 *Royal Society of London B Biological Sciences* **369**: 20130245.

567 Arnold SJ (1981). Behavioral Variation in Natural Populations. I. Phenotypic, Genetic and
568 Environmental Correlations Between Chemoreceptive Responses to Prey in the Garter
569 Snake, *Thamnophis*. *Evolution* **35**: 489–509.

570 Arnold SJ (1992). Constraints on Phenotypic Evolution. *American Naturalist* **140**: S85–S107.

571 Arnold SJ, Phillips PC (1999). Hierarchical comparison of genetic variance-covariance matrices.
572 II. Coastal-inland divergence in the garter snake, *Thamnophis elegans*. *Evolution* **53**: 1516–
573 1527.

574 Arnold SJ, Bürger R, Hohenlohe PA, Ajie BC, Jones AG (2008). Understanding the evoltuion
575 and stability of the G-matrix. *Evolution* **62**: 2451–2461.

576 Ashley-Ross MA, Perlman BM, Gibb AC, Long, Jr JH (2014). Jumping sans legs: does elastic
577 energy storage by the vertebral column power terrestrial jumps in bony fishes? *Zoology*,
578 117: 7-18.
579
580 Atchley WR, Rutledge JJ, Cowley DE (1981). Genetic Components of Size and Shape. II.
581 Multivariate Covariance Patterns in the Rat and. *Evolution* **35**: 1037–1055.

582 Austin PC, Hux JE (2002). A brief note on overlapping confidence intervals. Journal of Vascular
583 surgery 36:194-195.

584 Badyaev AV, Martin TE (2000). Individual variation in growth trajectories: phenotypic and
585 genetic correlations in ontogeny of the house finch. *Journal of Evolutionary Biology* **13**:
586 290–301.

587 Björklund, M (1997). Variation in growth in the blue tit (*Parus caeruleus*). *Journal of*
588 *Evolutionary Biology* **10**: 139–155.

589 Björklund M, Husby A, Gustafsson L (2013). Rapid and unpredictable changes of the G-matrix
590 in a natural bird population over 25 years. *Journal of Evolutionary Biology* **26**: 1–13.

591 Blumstein DT, Nguyen KT, Martin JGA (2013). Ontogenetic variation of heritability and
592 maternal effects in yellow-bellied marmot alarm calls. *Proceedings of the Royal Society B*

593 *Biological Sciences* **280**: 20130176.

594 Boulton K, Couto E, Grimmer AJ, Earley RL, Canario AVM, Wilson AJ, Walling CA (2015).
595 How integrated are behavioral and endocrine stress response traits? A repeated meaures
596 approach to testing the stress-coping style model. *Ecology and Evolution* **5**: 618-633.

597 Butler D (2009). asreml: asreml() fits the linear mixed model. R package version 3.0.
598 www.vsni.co.uk

599 Careau V, Wolak ME, Carter PA, Garland T (2015). Evolution of the additive genetic variance-
600 covariance matrix under continuous directional selection on a complex behavioural
601 phenotype. *Proceedings of the Royal Society B* **282**: 20151119.

602 Carrier DR (1983). Postnatal Ontogeny of the musculo-skeletal system in the Black-tailed jack
603 rabbit (*Lepus californicus*). *Journal of Zoology* **201***:* 27–55.

604 Charmantier A, Perrins C, McCleery RH, Sheldon BC (2006). Quantitative genetics of age at
605 reproduction in wild swans: support for antagonistic pleiotropy models of senescence.
606 *PNAS* **103**: 6587–6592.

607 Cheverud JM, Rutledge JJ, Atchley WR (1983). Quantitative Genetics of Development: Genetic
608 Correlations Among Age-Specific Trait Values and the Evolution of Ontogeny. *Evolution*
609 **37**: 895.

610 Cheverud JM (1988). A Comparison of Genetic and Phenotypic Correlations. *Evolution* **42**: 958-
611 968.

612 Cheverud JM (1995). Morphological Integration in the Saddle-Back Tamarin (*Saguinus*
613 *fuscicollis*) Cranium. *American Naturalist* **145**: 63-89.

614 Cheverud JM (1996). Developmental Integration and the Evolution of Pleiotropy. *American*
615 *Zoologist* **36**: 44–50.

616 Chevin L-M (2015). Evolution of adult size depends on genetic variance in growth trajectories: a
617 comment on analyses of evolutionary dynamics using integral projection models. *Methods*
618 *in Ecology and Evolution* **6**: 981-986.

619 Class B, Brommer JE (2015). A strong genetic correlation underlying a behavioural syndrome
620 disappears during development because of genotype –age interactions. *Proceedings of the*
621 *Royal Society B Biological Sciences* **282**: 20142777.

622 Cole KS, Noakes DLG (1997). Gonadal Development and Sexual Allocation in Mangrove
623 Killifish, *Rivulus marmoratus* (Pisces: Atherinomorpha). *Copeia* **1997**: 596-600.

624 Damián X, Fornoni J, Domínguez CA, Boege K (2017). Ontogenetic changes in the phenotypic

integration and modulatiry of leaf funcitonal traits. *Functional Ecology* **32**: 234-246.

Delahaie B, Charmantier A, Chantepie S, Garant D, Porlier M, Teplitsky C (2017). Conserved G-matrices of morphological and life-history traits among continenal and island blue tit populations. *Heredity* **119**: 76-87.

Earley RL, Hanninen AF, Fuller A, Garcia MJ, Lee EA (2012). Phenotypic plasticity and integration in the mangrove rivulus (*Kryptolebias marmoratus*): a prospectus. *Integrative and Comparative Biology* **52**: 814–827.

Ellis AG, Brockington SF, de Jager ML, Mellers G, Walker RH, Glover BJ (2014). Floral trait variation and integration as a fucntion of sexual deception in *Gorteria diffusa*. *Philosophical Transactions of the Royal Society of London B Biological Sciences* **369**: 20130563.

Eroukhmanoff F, Svensson EI (2008). Phenotypic integration and conserved covariance structure in calopterygid damselflies. *Journal of Evolutionary Biology* **21**: 514–526.

Fry JD (1992). The mixed-model analysis of variance applied to quantitative genetics: biological meaning of the parameters. *Evolution* **46**: 540–550.

Gibb AC, Ashley-Ross MA, Pace CM, Long JH (2011). Fish out of water: terrestrial jumping by fully aquatic fishes. *Journal of Experimental Zoology Part B Molecular and Developmental Evolution* **315A**: 649–653.

Gibb AC, Ashley-Ross MA, Hsieh ST (2013). Thrash, Flip, or Jump: The Behavioral and Functional Continuum of Terrestrial Locomotion in Teleost Fishes. *Integrative and Comparative Biology* **53**: 295–306.

Gignac PM, Santana SE (2016). A Bigger Picture: Organismal Function at the Nexus of Development, Ecology, and Evolution. *Integrative and Comparative Biology* **56**: 1-4.

Gilmour AR, Cullis BR, Gogel BJ, Welham SJ, Thompson R (2002). ASReml User Guide Release 1.0. *VSN Int Ltd*: 1–358.

Hadfield JD, Nutall A, Osorio D, Owens IPF (2007). Testing the phenotypic gambit: phenotypic, genetic, and environmental correlations of colour. *Journal of Evolutionary Biology* **20**: 549-557.

Hale ME (1999). Locomotor mechanics during early life history: effects of size and ontogeny on fast-start performance of salmonid fishes. *Journal of Experimental Biology* **202**: 1465-1479.

Herrel A, Gibb AC (2006). Ontogeny of Performance in Vertebrates. *Physiological and Biochemical Zoology* **79**: 1–6.

Houle D, Meyer K (2015). Estimating sampling error of evolutionary statistics based on genetic covariance matrices using maximum likelihood. *Journal of Evolutionary Biology* **28**: 1542-1549.

Houslay TM, Wilson AJ (2017). Avoiding the misuse of BLUP in behavioral ecology. *Behavioural Ecology* **28**: 948-952.

Huchard E, Charmantier A, English S, Bateman A, Nielsen JF, Clutton-Brock T (2014). Additive genetic variance and developmental plasticity in growth trajectories in a wild cooperative mammal. *Journal of Evolutionary Biology* **27**: 1893–1904.

Jokela J, Lively CM, Fox JA, Dybdahl MF (1997). Flat reation norms and "frozen" phenotypic variation in clonal snails (Potamopyrgus antipodarum). *Evolution* **5**: 1120-1129.

Kingsolver JG, Pfenning DW (2014). Patterns and power of phenotypic selection in nature. *BioScience* **57**(7): 561-572.

Klingenberg CP, Marugan-Lobon J (2013). Evolutionary Covariation in Geometric Morphometric Data: Analyzing Integration, Modularity, and Allometry in a Phylogenetic Context. *Systematic Biology* **62**: 591–610.

Klingenberg CP (2014). Studying morphological integration and modularity at multiple levels: concepts and analysis. *Philosophical Transactions of the Royal Society of London B Biological Science* **369**: 20130249.

Kruuk LEB, Slate J, Wilson AJ (2008). New Answers for Old Questions: The Evolutionary Quantitative Genetics of Wild Animal Populations. *Annual Review of Ecology Evolution and Systematics* **39**: 525-548.

Lande R (1979). Quantitative Genetic Analysis of Multivariate Evolution, Applied to Brain: Body Size Allometry. *Evolution* **33**: 402-416.

Lande R (1980). The genetic covariance between characters maintained by pleiotropic mutations. *Genetics* **94**: 203-215.

Lande R (1982). A quantitative genetic theory of life history evolution. *Ecology* **63**: 607-615.

Lande R, Arnold SJ (1983). The measurement of Selection on correlated characters. *Evolution* **37**: 1210–1226.

Leamy L, Cheverud JM (1984). Quantitative gentics and the evolution of ontogeny II. Genetic and environmental correlations among age-specific characters in random bred house mice. *Growth* **48**: 339-353.

Lofsvold D (1986). Quantitative Genetics of Morphological Differentiation in Peromyscus. I.

689 Tests of the Homogeneity of Genetic Covariance Structure Among Species and Subspecies.
690 *Evolution* **40**: 559–573.

691 Mabee PM, Olmstead KL, Cubbage CC (2000). An experimenal study of intraspecific variation,
692 developmental timing, and heterochrony in fishes. *Evolution* **54**: 2091–2106.

693 Mackiewicz M, Tatarenkov A, Perry A, Martin JR, Elder Jr. JF, Bechler DL, Avise JC (2006).
694 Microsatellite documentation of male-mediated outcrossing between inbred laboratory
695 strains of the self-fertilizing mangrove killifish (*Kryptolebias marmoratus*). *Journal of*
696 *Heredity* **97**: 508-513.

697 Magellan K (2016) Amphibious adaptations in a newly recognized amphibious fish: Terrestrial
698 locomotion and the influences of body size and temperature. *Austral Ecology* **41**: 446-454.

699 Margres MJ, Wray KP, Seavy M, McGivern JJ, Sanader D, Rokyta DR (2015). Phenotypic
700 integration in the feeding system of the eastern diamondback rattlesnake (*Crotalus*
701 *adamanteus*). *Molecular Ecology* **24**: 3405–3420.

702 Marroig G, Cheverud JM (2001). A comparison of phenotypic variation and covariation patterns
703 and the role of phylogeny, ecology, and ontogeny during cranial evoltuion of new world
704 monkeys. *Evolution* **55**: 2576–2600.

705 Marroig G, Cheverud JM (2005). Size as a Line of Least Evolutionary Resistance: Diet and
706 Adaptive Morphological Radiation in New World Monkeys. *Evolution* **59**: 1128–1142.

707 Mitteroecker P, Bookstein F (2009). The ontogenetic trajectory of the phenotypic covariance
708 matrix, with examples from craniofacial shape in rats and humans. *Evolution* **63**: 727–737.

709 Moran NA (1994). Adaptation and constraints in the complex life-cycles of animals. *Annu Rev*
710 *Ecology Evolution and Systematics* **25**: 573–600.

711 Negovetic S, Jokela J (2001). Life-history variation, phenotypic plasticity, and subpopulation
712 structure in a freshwater snail. *Ecology* **82**: 2805-2815.

713 Niklasson M, Tomiuk J, Parker Jr. ED (2004). Maintanence of clonal diversity in Dipsa bifurcata
714 (Fallén, 1810) (Diptera: Lonchopteridae). I. Flucutating seasonal selection moulds long-
715 term coexistence. *Heredity* **93**: 62-71.

716 Nilsson-Örtman VN, Rogell B, Stoks R, Johansson F (2015). Ontogenetic changes in genetic
717 variances of age-dependent plasticity along a latitudinal gradient. *Heredity* **115**: 366–378.

718 Pantel JH, Juenger TE, Leibold MA (2011). Environmental gradients structure Daphnia pulex x
719 pulicaria clonal distribution. *Journal of Evolutionary Biology* **24**: 723-732.

720 Penna A, Melo D, Bernardi S, Oyarzabal MI, Marroig G (2017). The evolution of phenotypic
721 integration: How directional selection reshapes covariation in mice. *Evolution* **71**: 2370-
722 2380.

723 Perez-Barrales R, Simon-Porcar VI, Santos-Gally R, Arroyo J (2014). Phenotypic integration in
724 style dimorphic daffodils (Narcissus, Amaryllidaceae) with different pollinators.
725 *Philosophical Transactions of the Royal Society of London B Biological Science* **369**:
726 20130258.

727 Perlman BM, Ashley-Ross MA (2016). By land or by sea: a modified C-start motor pattern
728 drives the terrestrial tail-flip. Journal of Experimental Biology 219:1860-1865.

729 Pigliucci M (2003) Phenotypic integration: studying the ecology and evolution of complex
730 phenotypes. *Ecology Letters* **6**: 265-272.

731 Porto A, De Oliveira FB, Shirai LT, DeConto, Marroig G (2009). The Evolution of Modularity
732 in the Mammalian Skull I: Morphological Integration Patterns and Magnitudes.
733 *Evolutionary Biology* **36**: 118-135.

734 R Core Team (2017). R: A language and environment for statistical computing. R Foundation for
735 Statistical Computing, Vienna, Austria. URL https://www.R-project.org/.

736 Roff DA, Wilson AJ (2014). Quantifying genetic by environmental interactions in laboratory
737 systems. In: Hunt J, Hosken DJ (eds.) *Genotype by environment interactions and sexual*
738 *selection*, Wiley-Blackwell: New Jersey.

739 Scarsella G, Gresham JD, Earley RL (2017). Relationships between external sexually dimorphic
740 characteristics and internal gondal morphology in the sex changing fish, Kryptolebias
741 marmoratus. *Journal of Zoology*, DOI: 10.1111/jzo.12546.

742 Schluter D (1996). Adaptive radiation along genetic lines of least resistance. *Evolution*
743 **50**(5):1766-1174.

744 Schneider CA, Rasband WS, Eliceiri KW (2012). NIH Image to ImageJ: 25 years of image
745 analysis. *Nature methods* **9**(7): 671-675.

746 Steppan SJ, Phillips PC, Houle D (2002). Comparative quantitative genetics: evolution of the G-
747 matrix. *Trends in Ecology and Evolution* **17**: 320-327.

748 Styga JM, Houslay TM, Wilson AJ, Early RL (2018). Ontogeny of the morphology-performance
749 axis in an amphibious fish (*Kryptolebias marmoratus)*. *Journal of Experimental Zoology*,
750 *Part A*, DOI: 10.1002/jez.2150.

751 Tatarenkov A, Lima SMQ, Avise JC (2011). Extreme homogeneity and low genetic diversity in
752 Kryptolebias ocellatus from south-eastern Brazil suggest a recent foundation for this

androdioecious fish population. *Journal of Fish Biology* **79**: 2095–2105.

Taylor DS (2012). Twenty-Four Years in the Mud: What Have We Learned About the Natural History and Ecology of the Mangrove Rivulus, *Kryptolebias marmoratus*? *Integrative and Comparative Biology* **52**: 724–736.

Trillmich F, Bieneck M, Geissler E, Bischof H-J (2003). Ontogeny of running performance in the wild guinea pig (Cavia aperea). *Mammalian Biology* **68**: 214–223.

Turner BJ, Davis WP, Taylor DS (1992). Abundant males in populations of a selfing hermaphrodite fish, Rivulus marmoratus, from some Belize cays. *Journal of Fish Biology* **40**: 307-310.

Visscher PM (2006). A note on the asymptotic distribution of likelihood ratio tests to test variance components. *Twin Research in Human Genetics* **9:** 490-495.

Walsh B, Blows MW (2009). Abundant genetic variation + strong selection = mutlivariate genetic constraints: A geometric view of adaptation. *Annual Review of Ecology, Evolution, and Systematics* **40**: 41-59.

Watkins TB (2001). A quantitative genetic test of adaptive decoupling across metamorphosis for locomotor and life-history traits in the pacific tree frog, Hyla regilla. *Evolution* **55**: 1668–1677.

Webb GN, Byrd RA (1994). Simultaneous Differential Staining of Cartilage and Bone in Rodent Fetuses: an Alcian Blue and Alizarin Red S Procedure without Glacial Acetic Acid. *Biotechnology and Histochemistry* **69**: 181–185.

Wilson AJ, Charmatier A, Hadfield JD (2008). The Evolutionary Ecology of senescence: Evolutionary genetics of adeing in the wild: empirical partterns and future perspectives. *Functional Ecology* **22**: 431-442.

Fig. 1: Variation in overall phenotypic variance (Trace of the P matrix), overall genetic variance (Trace of the G-matrix; variance scale), overall heritability (Trace of the G-matrix; heritability scale), phenotypic integration (mean squared correlation, P-matrix), and genetic integration (mean squared correlation, G-matrix) across ages (1, 15, and 100 DPH). Confidence intervals are generated from 5,000 bootstrap draws. Estimates are significantly different when 95% confidence intervals do not overlap. Also included are representative pictures of each age class with scale bars.

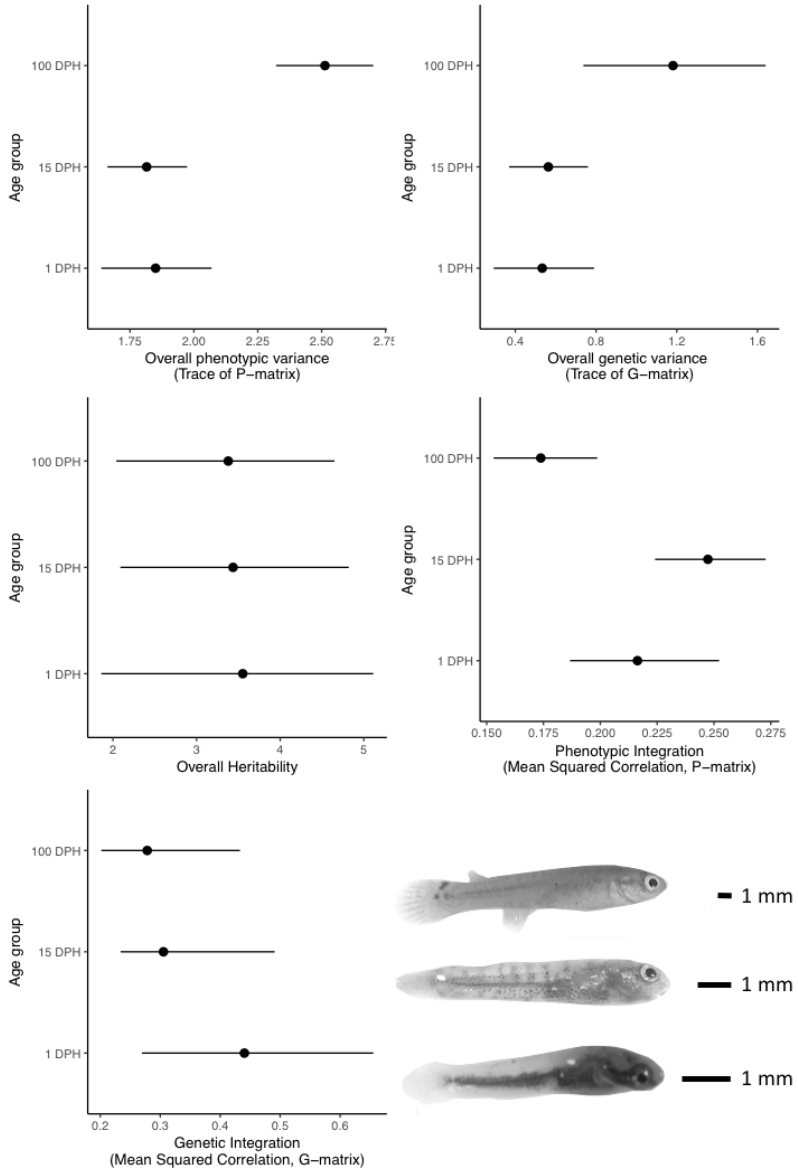

Fig. 2: Pairwise-trait phenotypic correlations (rP, below diagonal) and pairwise-trait genetic correlations (rG, above diagonal) for 1, 15, and 100 DPH. Correlations are color coded by strength and direction. Correlations shown in blue are positive and correlations shown in red are negative. Stronger correlations are indicated by narrower ellipses, while weaker correlations are indicated by ellipses approaching a spherical shape. EPL=Epural length, EPA=Epural angle, PHPL=parahypural length, PHPA=parahypural angle, HYPL=hypural length, HYPW=hypural width, and SL=standard length.

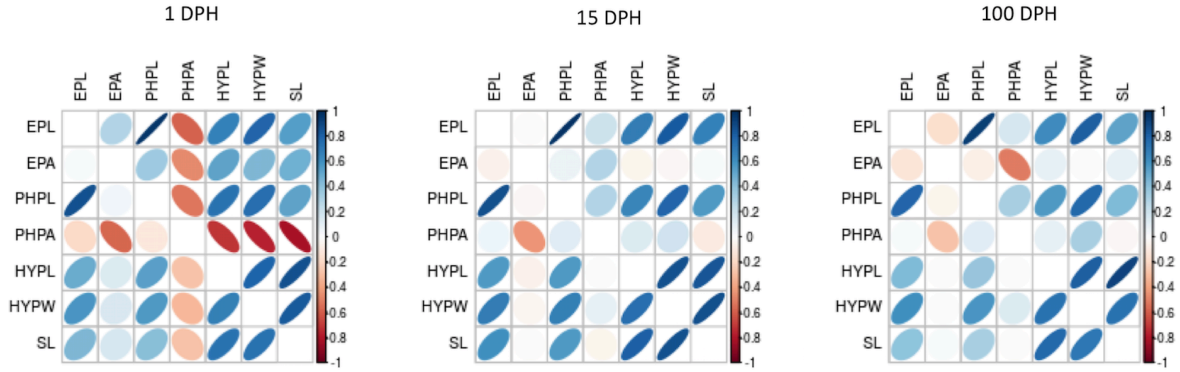

Fig. 3: Difference matrices for pairwise-trait phenotypic correlations (rP, below diagonal) and pairwise-trait genetic correlations (rG, above diagonal) from 1, 15, and 100 DPH. Differences are color coded by strength and direction. Differences shown in blue are positive and differences shown in red are negative. When ages are similar, the colored square is small; when ages are very different, the colored square fills the cell. EPL=Epural length, EPA=Epural angle, PHPL=parahypural length, PHPA=parahypural angle, HYPL=hypural length, HYPW=hypural width, and SL=standard length.

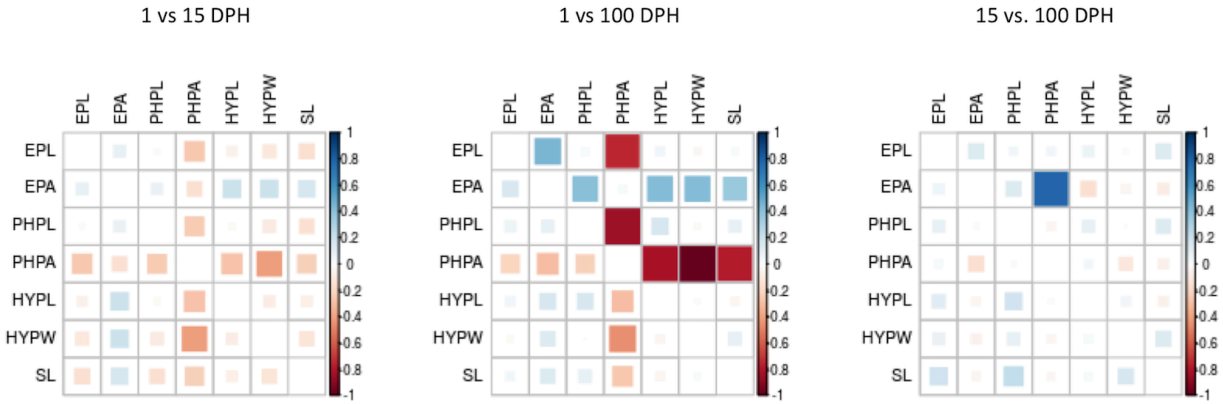

Table 1: Phenotypic variance (V_p), genetic variance (V_G; variance scale), and genetic variance (H^2; heritability scale) for each trait at 1, 15, and 100 DPH. EPL=Epural length, EPA=Epural angle, PHPL=parahypural length, PHPA=parahypural angle, HYPL=hypural length, HYPW=hypural width, and SL=standard length.

	1 DPH			15 DPH			100 DPH		
Trait	**V_P** ***(CI)***	**V_G** ***(CI)***	**H^2** ***(CI)***	**V_P** ***(CI)***	**V_G** ***(CI)***	**H^2** ***(CI)***	**V_P** ***(CI)***	**V_G** ***(CI)***	**H^2** ***(CI)***
EPL	0.06 *(0.05, 0.07)*	0.05 *(0.02, 0.08)*	0.48 *(0.21, 0.76)*	0.16 *(0.13, 0.18)*	0.11 *(0.05, 0.18)*	0.73 *(0.36, 1.12)*	0.44 *(0.37, 0.50)*	0.3 *(0.14, 0.45)*	0.66 *(0.29, 0.98)*
EPA	0.68 *(0.57, 0.78)*	0.18 *(0.05, 0.31)*	0.13 *(0.04, 0.22)*	0.66 *(0.57, 0.76)*	0.06 *(0.01, 0.12)*	0.1 *(0.01, 0.19)*	0.49 *(0.42, 0.56)*	0.09 *(0.03, 0.16)*	0.15 *(0.05, 0.26)*
PHPL	0.06 *(0.05, 0.07)*	0.05 *(0.02, 0.08)*	0.40 *(0.16, 0.62)*	0.14 *(0.12, 0.16)*	0.11 *(0.05, 0.16)*	0.75 *(0.36, 1.14)*	0.4 *(0.35, 0.47)*	0.3 *(0.15, 0.4)*	0.69 *(0.32, 1.05)*
PHPA	0.95 *(0.81, 1.11)*	0.18 *(0.04, 0.31)*	0.10 *(0.02, 0.18)*	0.63 *(0.53, 0.72)*	0.16 *(0.07, 0.27)*	0.24 *(0.09, 0.39)*	0.46 *(0.4, 0.53)*	0.01 *(-0.03, 0.05)*	0.12 *(0.02, 0.21)*
HYPL	0.05 *(0.04, 0.05)*	0.04 *(0.02, 0.06)*	0.81 *(0.36, 1.28)*	0.1 *(0.08, 0.11)*	0.04 *(0.02, 0.07)*	0.46 *(0.20, 0.72)*	0.27 *(0.23, 0.31)*	0.13 *(0.05, 0.21)*	0.5 *(0.21, 0.76)*
HYPW	0.03 *(0.03, 0.04)*	0.02 *(0.01, 0.04)*	0.76 *(0.34, 1.19)*	0.07 *(0.06, 0.08)*	0.04 *(0.02, 0.06)*	0.58 *(0.26, 0.89)*	0.31 *(0.27, 0.35)*	0.2 *(0.09, 0.30)*	0.66 *(0.31, 1.03)*
SL	0.02 *(0.01, 0.02)*	0.01 *(0.01, 0.02)*	0.88 *(0.35, 1.35)*	0.06 *(0.05, 0.07)*	0.04 *(0.02, 0.06)*	0.58 *(0.28, 0.90)*	0.15 *(0.13, 0.18)*	0.09 *(0.05, 0.14)*	0.6 *(0.28, 0.94)*

Table 2: Differences in phenotypic variance (V_p), genetic variance (V_G; variance scale), and genetic variance (H^2; heritability scale) for each trait between 1 and 15 DPH, 1 and 100 DPH, and 15 and 100 DPH. Asterisks indicate significant differences in V_P, V_G, or H^2 between the age groups shown in the header. EPL=Epural length, EPA=Epural angle, PHPL=parahypural length, PHPA=parahypural angle, HYPL=hypural length, HYPW=hypural width, and SL=standard length.

	1 vs 15 DPH			1 vs 100 DPH			15 vs 100 DPH		
Trait	**V_P** ***(CI)***	**V_G** ***(CI)***	**H^2** ***(CI)***	**V_P** ***(CI)***	**V_G** ***(CI)***	**H^2** ***(CI)***	**V_P** ***(CI)***	**V_G** ***(CI)***	**H^2** ***(CI)***
EPL	-0.1* *(-0.12, -0.07)*	-0.06 *(-0.13, 0.001)*	-0.25 *(-0.71, 0.22)*	-0.37* *(-0.44, -0.31)*	-0.25* *(-0.41, -0.09)*	-0.17 *(-0.64, 0.23)*	-0.28* *(-0.35, -0.21)*	-0.19* *(-0.36, -0.02)*	*0.07* *(-0.44, 0.59)*
EPA	0.02 *(-0.12, 0.20)*	0.11 *(-0.01, 0.26)*	0.04 *(-0.09, 0.16)*	0.19* *(0.07, 0.33)*	0.09 *(-0.05, 0.23)*	-0.02 *(-0.16, 0.12)*	0.18* *(0.05, 0.29)*	-0.03 *(-0.12, 0.06)*	*-0.06* *(-0.19, 0.08)*
PHPL	-0.08* *(-0.1, -0.05)*	-0.05 *(-0.12, 0.01)*	-0.35 *(-0.82, 0.09)*	-0.33* *(-0.04, -0.29)*	-0.24* *(-0.41, -0.09)*	-0.29 *(-0.71, 0.15)*	-0.26* *(-0.32, -0.2)*	-0.19* *(-0.36, -0.04)*	*0.06* *(-0.51, 0.57)*
PHPA	0.32* *(0.15, 0.50)*	0.02 *(-0.16, 0.18)*	-0.14 *(-0.31, 0.04)*	0.49* *(0.33, 0.66)*	0.11 *(-0.03, 0.26)*	-0.02 *(-0.13, 0.12)*	0.17* *(0.06, 0.28)*	0.1 *(-0.01, 0.21)*	*0.12* *(-0.06, 0.30)*
HYPL	-0.05* *(-0.07, -0.04)*	-0.01 *(-0.04, 0.03)*	0.35 *(-0.18, 0.91)*	-0.21* *(-0.26, -0.18)*	-0.1* *(-0.17, -0.02)*	0.31 *(-0.27, 0.84)*	-0.16* *(-0.21, -0.13)*	-0.09* *(-0.16, -0.01)*	*-0.03* *(-0.42, 0.34)*
HYPW	-0.04* *(-0.05, -0.03)*	-0.01 *(-0.04, 0.01)*	0.18 *(-0.25, 0.70)*	-0.27* *(-0.32, -0.23)*	-0.18* *(-0.29, -0.07)*	0.1 *(-0.44, 0.66)*	-0.24* *(-0.29, -0.2)*	-0.2* *(-0.27, -0.05)*	*-0.08* *(-0.55, 0.40)*
SL	-0.04* *(-0.06, -0.04)*	-0.02* *(-0.04, -0.002)*	0.29 *(-0.30, 0.85)*	-0.14* *(-0.16, -0.12)*	-0.08* *(-0.13, -0.03)*	0.27 *(-0.37, 0.83)*	-0.09* *(-0.12, -0.07)*	-0.06* *(-0.11, -0.004)*	*-0.02* *(-0.45, 0.45)*

Table 3: Likelihood ratio tests of genetic variance and genotype x age (GxA) interactions for each morphological trait. Also shown are the genetic correlations between each pair of ages (+/- 1.96*SE) estimated under the GxA model. Asterisks denote significant correlations between ages. EPL=Epural length, EPA=Epural angle, PHPL=parahypural length, PHPA=parahypural angle, HYPL=hypural length, HYPW=hypural width, and SL=standard length.

Trait	**Genetic Variance**			**GxA**			**Between age genetic correlations**		
	χ^2	DF	p-value	χ^2	DF	p-value	1 DPH vs 15 DPH	1 DPH vs 100 DPH	15 DPH vs 100 DPH
EPL	377.2	1	<0.001	572.0	5	<0.001	-0.07 (-0.1 to -0.04)*	0.18 (0.12 to 0.24)*	-0.37 (-0.46 to -0.28)*
EPA	42.2	1	<0.001	45.6	5	<0.001	0.19 (0.09 to 0.29)*	0.24 (0.12 to 0.36)*	-0.12 (-0.2 to -0.04)*
PHPL	331.9	1	<0.001	633.3	5	<0.001	-0.02 (-0.06 to 0.02)	0.06 (0.003 to 0.12)*	-0.31 (-0.4 to -0.22)*
PHPA	64.25	1	<0.001	41.6	5	<0.001	0.45 (0.33 to 0.57)*	0.10 (0.01 to 0.19)*	0.29 (0.21 to 0.37)*
HYPL	238.5	1	<0.001	337.6	5	<0.001	0.05 (0.03 to 0.07)*	-0.42 (-0.46 to -0.38)*	-0.29 (-0.33 to -0.25)*
HYPW	365.7	1	<0.001	441.0	5	<0.001	-0.001 (-0.01 to 0.01)	-0.58 (-0.62 to -0.54)*	-0.28 (-0.32 to -0.24)*
SL	418.4	1	<0.001	436.8	5	<0.001	-0.004 (-0.01 to 0.01)	-0.07 (-0.09 to -0.05)*	-0.03 (-0.06 to -0.002)*

Table S1: Number of individuals acquired for each age group and genotype combination. Generations (Gen) of individuals are also given for each genetic line. The number of microsatellite loci at which the wild-caught progenitor of these animals was homozygous are shown in parentheses next to the genotype name.

Genotype	Gen	1 DPH	15 DPH	100 DPH	Genotype	Gen	1 DPH	15 DPH	100 DPH
BP11 (32)	F3/F4			12	NUKE5 (27)	F3	10	11	10
BP15 (31)	F3/F4	10	11		NUKE9 (32)	F3	16	15	14
BP18 (32)	F3			13	OSR7 (32)	F2	15	14	13
BP23 (32)	F2/F3	14	14	15	OSR9 (32)	F2	15	14	14
BP4 (32)	F3/F4		10		RAD1 (32)	F2	10	13	12
BWS21 (30)	F2/F3			13	RAD13 (32)	F2	13	11	14
BWS38 (25)	F2/F3		10		RAD6 (32)	F3		8	
CROC22 (30)	F2			10	RHL (32)	F12	14	13	16
CROC27 (22)	F2		11		RHL2 (32)	F2	12	10	10
CRWL18 (32)	F2			11	RHL3 (32)	F2	24	12	13
CRWL19 (32)	F2			10	RHL5 (32)	F2	15	11	
DC22 (32)	F3	14	15	12	RHL6 (31)	F2	11	12	
DC8 (16)	F2	12	13	15	RHL9 (32)	F2	12		
FW6 (32)	F2	11	13		RHL7 (32)	F2	10	12	
HAM9 (32)	F2			10	SAND20 (24)	F2			10
LMC1 (29)	F2	11	13	10	SAND21(30)	F2			10
MES14 (32)	F2			11	SAX14 (32)	F2		12	10
MRT8 (32)	F2		10		SAX7 (32)	F2	10	11	
NEL1 (32)	F2	12	14	13	SOB9 (29)	F2	12	11	10
NEL10 (32)	F2	11		13	UM2 (30)	F2	10	12	14
NUKE13 (32)	F2		11		WEED10 (32)	F2			10
NUKE2 (32)	F2	10	13	11	WEED4 (31)	F2	13	11	10

 # Genotypes: I DPH (N=30), 15 DPH (N=34), 100 DPH (N=35)

 # Individuals: 1 DPH (N=324), 15 DPH (N=368), 100 DPH (N=368)

Table S2: Clearing and Staining Time Protocol. Specimens were first placed in a 1:1:18 staining solution of 0.1% Alcian blue: 0.2% Alizarin red S: 70% EtOH. Forty grams of potassium hydrogen phthalate was added to this solution to stabilize the pH between 5.2-5.8. Specimens were then transferred to a 1% KOH solution, followed by a 2:2:1 solution of glycerol: 70% EtOH: benzyl alcohol. Finally, specimens were stored in a 1:1 solution of glycerol and 70% EtOH. Durations for each stage of the process are shown.

Age	**Stain**	**KOH**	**2:2:1**
1 DPH	24 hours	1 hour	1 hour
15 DPH	48 hours	2 hours	1 hour
100 DPH	72 hours	10 hours	14 hours

Table S3: The fixed effect of 'Time' (i.e. interval [days] between hatching date and laid date) on morphological structure when: 1.) phenotypic variance/covariance matrices (**P**-matrices) were estimated across all traits at each age, and 2.) genetic variance/covariance matrices (**G**-matrices) were estimated across all traits at each age. EPL=Epural length, EPA=Epural angle, PHPL=parahypural length, PHPA=parahypural angle, HYPL=hypural length, HYPW=hypural width, and SL=standard length.

		1 DPH			15 DPH			100 DPH		
	Response trait	Slope	Wald's $F_{(Num, Den DF)}$	P	Slope	Wald's $F_{(Num, Den DF)}$	P	Slope	Wald's $F_{(Num, Den DF)}$	P
P-matrix	EPA	0.002	F (7, 2176)=4.4	P=<0.001*	0.002	F (7,2553)=2.2	P=0.04*	-0.009	F (7, 2534)=2.7	P=0.008*
	EPL	0.002			-0.003			0.0004		
	HYPL	-0.006			-0.007			-0.007		
	HYPW	-0.0005			-0.01			-0.001		
	PHPA	-0.009			-0.01			-0.006		
	PHPL	-0.006			0.0004			-0.002		
	SL	-0.02			-0.008			-0.009		
G-matrix	EPA	0.004	F (7,2148)=1.9	P=0.07	0.004	F (7, 2525)=0.80	P=0.59	-0.003	F (7, 2506)=1.1	P=0.38
	EPL	-0.0005			0.0004			0.001		
	HYPL	0.003			-0.002			-0.00005		
	HYPW	0.004			0.0006			0.0008		
	PHPA	-0.009			-0.006			-0.008		
	PHPL	-0.006			0.001			-0.0003		
	SL	-0.002			0.003			-0.003		

Table S4: Differences in phenotypic variance ('Trace') and integration between each age group. Differences in genetic variance ('Trace' (variance scale)), heritability ('Trace' (heritability scale)), and integration between each age group. Integration was estimated by the mean squared correlation across all traits. Significance based on 95% CI generated from 5,000 bootstrap estimates is indicated by an asterisk. Significant differences are noted when 95% CI do not span zero.

Matrix	**Comparison**	**Age comparison**	**95% CI of difference**
P	Trace	1 vs. 15	-0.23 to 0.29
		1 vs. 100	-0.94 to -0.37*
		15 vs. 100	-0.94 to -0.45*
	Integration (mean squared correlation)	1 vs. 15	-0.07 to 0.008
		1 vs. 100	0.002 to 0.08*
		15 vs. 100	0.04 to 0.11*
G	Trace (variance scale)	1 vs. 15	-0.33 to 0.29
		1 vs. 100	-1.13 to -0.16*
		15 vs. 100	-1.14 to -0.13*
	Trace (heritability scale)	1 vs. 15	-1.96 to 2.14
		1 vs. 100	-1.85 to 2.17
		15 vs. 100	-1.90 to 1.94
	Integration (mean squared correlation)	1 vs. 15	-0.11 to 0.26
		1 vs. 100	-0.088 to 0.38
		15 vs. 100	-0.16 to 0.22

Table S5: Age dependent phenotypic variance-covariance and correlation matrices (**P**) for: 1, 15, and 100 DPH ages. Phenotypic variance estimates are shown in bold on the diagonal, covariances are shown in shaded cells below the diagonals, and correlations above the diagonal. Approximate 95% CI are shown in parentheses and asterisks denote nominally significant correlations. EPL=Epural length, EPA=Epural angle, PHPL=parahypural length, PHPA=parahypural angle, HYPL=hypural length, HYPW=hypural width, and SL=standard length.

1 DPH	EPL	EPA	PHPL	PHPA	HYPL	HYPW	SL
EPL	**0.06 (0.05,0.07)**	0.03 (-0.09,0.14)	0.86 (0.83,0.89)*	-0.19 (-0.3,-0.08)*	0.49 (0.4,0.57)*	0.57 (0.5,0.65)*	0.44 (0.36,0.53)*
EPA	0.01 (-0.02,0.03)	**0.68 (0.57,0.78)**	0.04 (-0.07,0.15)	-0.57 (-0.65,-0.5)*	0.14 (0.04,0.26)*	0.16 (0.04,0.27)*	0.16 (0.05,0.27)*
PHPL	0.05 (0.05,0.06)	0.01 (-0.01,0.03)	**0.06 (0.05,0.07)**	-0.12 (-0.22,-0.008)*	0.54 (0.46,0.62)*	0.57 (0.49,0.64)*	0.42 (0.33,0.51)*
PHPA	-0.05 (-0.07,-0.02)	-0.46 (-0.56,-0.35)	-0.03 (-0.06,0)	**0.95 (0.81,1.11)**	-0.28 (-0.38,-0.17)*	-0.32 (-0.42,-0.22)*	-0.28 (-0.39,-0.19)*
HYPL	0.03 (0.02,0.03)	0.03 (0.01,0.05)	0.03 (0.02,0.04)	-0.06 (-0.08,-0.03)	**0.05 (0.04,0.05)**	0.68 (0.62,0.74)*	0.73 (0.68,0.78)*
HYPW	0.03 (0.02,0.03)	0.02 (0.01,0.04)	0.03 (0.02,0.03)	-0.06 (-0.08,-0.04)	0.03 (0.02,0.03)	**0.03 (0.03,0.04)**	0.74 (0.68,0.78)*
SL	0.01 (0.01,0.02)	0.02 (0.01,0.03)	0.01 (0.01,0.02)	-0.03 (-0.05,-0.02)	0.02 (0.02,0.02)	0.02 (0.01,0.02)	**0.02 (0.01,0.02)**

15 DPH	EPL	EPA	PHPL	PHPA	HYPL	HYPW	SL
EPL	**0.16 (0.13,0.18)**	-0.06 (-0.17,0.04)	0.88 (0.86,0.9)*	0.06 (-0.04,0.16)	0.56 (0.49,0.63)*	0.68 (0.63,0.74)*	0.59 (0.53,0.66)*
EPA	-0.02 (-0.05,0.01)	**0.66 (0.57,0.76)**	-0.04 (-0.14,0.06)	-0.43 (-0.51,-0.35)*	-0.06 (-0.17,0.04)	-0.05 (-0.15,0.06)	-0.02 (-0.12,0.09)
PHPL	0.13 (0.11,0.15)	-0.01 (-0.04,0.02)	**0.14 (0.12,0.16)**	0.13 (0.02,0.22)*	0.56 (0.5,0.63)*	0.67 (0.61,0.73)*	0.56 (0.49,0.63)*
PHPA	0.02 (-0.01,0.05)	-0.28 (-0.35,-0.21)	0.04 (0.01,0.07)	**0.63 (0.53,0.72)**	0 (-0.11,0.1)	0.09 (-0.01,0.19)	-0.06 (-0.16,0.04)
HYPL	0.07 (0.05,0.08)	-0.02 (-0.04,0.01)	0.07 (0.05,0.08)	0 (-0.03,0.02)	**0.1 (0.08,0.11)**	0.76 (0.71,0.8)*	0.8 (0.77,0.84)*
HYPW	0.07 (0.06,0.08)	-0.01 (-0.03,0.01)	0.07 (0.05,0.08)	0.02 (0,0.04)	0.06 (0.05,0.07)	**0.07 (0.06,0.08)**	0.87 (0.84,0.89)*
SL	0.06 (0.05,0.07)	0 (-0.02,0.02)	0.05 (0.04,0.06)	-0.01 (-0.03,0.01)	0.06 (0.05,0.07)	0.06 (0.05,0.07)	**0.06 (0.05,0.07)**

100 DPH	EPL	EPA	PHPL	PHPA	HYPL	HYPW	SL
EPL	**0.44 (0.37,0.5)**	-0.13 (-0.23,-0.03)*	0.79 (0.75,0.83)*	0.03 (-0.08,0.13)	0.44 (0.35,0.52)*	0.6 (0.52,0.66)*	0.4 (0.31,0.48)*
EPA	-0.06 (-0.11,-0.01)	**0.49 (0.42,0.56)**	-0.05 (-0.16,0.05)	-0.28 (-0.37,-0.18)*	-0.02 (-0.12,0.08)	0.02 (-0.09,0.11)	0.03 (-0.08,0.13)
PHPL	0.33 (0.27,0.39)	-0.02 (-0.07,0.02)	**0.4 (0.35,0.47)**	0.11 (0.01,0.21)*	0.38 (0.28,0.46)*	0.57 (0.5,0.64)*	0.32 (0.22,0.41)*
PHPA	0.01 (-0.03,0.06)	-0.13 (-0.18,-0.08)	0.05 (0,0.09)	**0.46 (0.4,0.53)**	0.02 (-0.08,0.12)	0.14 (0.04,0.24)*	-0.02 (-0.12,0.09)
HYPL	0.15 (0.11,0.19)	-0.01 (-0.04,0.03)	0.12 (0.09,0.16)	0.01 (-0.03,0.04)	**0.27 (0.23,0.31)**	0.72 (0.67,0.77)*	0.77 (0.73,0.81)*
HYPW	0.22 (0.18,0.26)	0.01 (-0.04,0.04)	0.2 (0.16,0.24)	0.05 (0.01,0.09)	0.21 (0.17,0.24)	**0.31 (0.27,0.35)**	0.71 (0.66,0.76)*
SL	0.1 (0.07,0.13)	0.01 (-0.02,0.04)	0.08 (0.05,0.1)	-0.01 (-0.03,0.02)	0.16 (0.13,0.18)	0.16 (0.13,0.18)	**0.15 (0.13,0.18)**

Table S6: Estimated differences (with approximate 95% CI in parentheses) between each pair of ages in phenotypic variances (bold font, diagonal) and correlations (above diagonal). For each of these differences, the second age was subtracted from the first so a negative value reflects a higher value in an older age relative to a younger age. Asterisks denote significant differences in age specific parameters as evidenced by confidence intervals that do not span zero. EPL=Epural length, EPA=Epural angle, PHPL=parahypural length, PHPA=parahypural angle, HYPL=hypural length, HYPW=hypural width, and SL=standard length.

1 vs 15 DPH	EPL	EPA	PHPL	PHPA	HYPL	HYPW	SL
EPL	**-0.1 (-0.12, -0.07)***	0.09 (-0.07,0.24)	-0.02 (-0.05,0.02)	-0.26 (-0.41,-0.1)*	-0.06 (-0.17,0.05)	-0.11 (-0.2,-0.02)*	-0.15 (-0.26,-0.03)*
EPA		**0.02 (-0.12, 0.2)**	0.08 (-0.08,0.23)	-0.14 (-0.25,-0.03)*	0.21 (0.05,0.35)*	0.2 (0.05,0.34)*	0.18 (0.03,0.33)*
PHPL			**-0.08 (-0.1, -0.05)***	-0.24 (-0.4,-0.09)*	-0.03 (-0.13,0.07)	-0.1 (-0.2,-0.01)*	-0.14 (-0.26,-0.02)*
PHPA				**0.32 (0.15, 0.5)***	-0.28 (-0.43,-0.13)*	-0.41 (-0.55,-0.26)*	-0.23 (-0.38,-0.09)*
HYPL					**-0.05 (-0.07, -0.04)***	-0.08 (-0.16,-0.01)*	-0.08 (-0.14,-0.02)*
HYPW						**-0.04 (-0.05, -0.03)***	-0.13 (-0.19,-0.07)*
SL							**-0.04 (-0.06, -0.04)***

1 vs 100 DPH	EPL	EPA	PHPL	PHPA	HYPL	HYPW	SL
EPL	**-0.37 (-0.44, -0.31)***	0.16 (0.01,0.32)*	0.07 (0.03,0.13)*	-0.22 (-0.37,-0.07)*	0.06 (-0.07,0.17)	-0.02 (-0.12,0.08)	0.05 (-0.08,0.17)
EPA		**0.19 (0.07, 0.33)***	0.1 (-0.06,0.24)	-0.29 (-0.42,-0.17)*	0.16 (0.01,0.31)*	0.14 (-0.01,0.29)	0.14 (-0.02,0.27)
PHPL			**-0.33 (-0.4, -0.29)***	-0.23 (-0.37,-0.08)*	0.16 (0.04,0.28)*	-0.005 (-0.1,0.1)	0.1 (-0.03,0.23)
PHPA				**0.49 (0.33, 0.66)***	-0.3 (-0.44,-0.14)*	-0.46 (-0.59,-0.31)	-0.26 (-0.41,-0.12)
HYPL					**-0.21 (-0.26, -0.18)***	-0.05 (-0.12,0.03)	-0.05 (-0.11,0.02)
HYPW						**-0.27 (-0.32, -0.23)***	0.02 (-0.05,0.09)
SL							**-0.14 (-0.16, -0.12)***

15 vs 100 DPH	EPL	EPA	PHPL	PHPA	HYPL	HYPW	SL
EPL	**-0.28 (-0.35, -0.21)***	0.07 (-0.07,0.22)	0.09 (0.05,0.14)*	0.04 (-0.11,0.18)	0.12 (0.01,0.23)*	0.09 (0.003,0.17)	0.2 (0.09,0.31)
EPA		**0.18 (0.05, 0.29)***	0.02 (-0.14,0.15)	-0.15 (-0.28,-0.02)*	-0.04 (-0.18,0.1)	-0.06 (-0.21,0.08)	-0.04 (-0.19,0.1)
PHPL			**-0.26 (-0.32, -0.2)***	0.02 (-0.13,0.15)	0.19 (0.07,0.3)*	0.1 (0.01,0.19)	0.24 (0.13,0.36)
PHPA				**0.17 (0.06, 0.28)***	-0.02 (-0.16,0.13)	-0.04 (-0.19,0.1)	-0.04 (-0.18,0.11)
HYPL					**-0.16 (-0.21, -0.13)***	0.04 (-0.03,0.1)	0.03 (-0.03,0.08)
HYPW						**-0.24 (-0.29, -0.2)***	0.16 (0.1,0.21)
SL							**-0.09 (-0.12, -0.07)***

Table S7: Age dependent genetic variance-covariance and correlation matrices (**G**) for: 1, 15, and 100 DPH ages. Genetic variances are shown in bold font on the diagonal with estimates on the 'heritability scale' underneath (italic font, see text for details). Genetic covariances are shown in shaded cells below the diagonal, and corresponding genetic correlations are shown above the diagonal. Approximate 95% CI are shown in parentheses and asterisks denote nominally significant genetic correlations. EPL=Epural length, EPA=Epural angle, PHPL=parahypural length, PHPA=parahypural angle, HYPL=hypural length, HYPW=hypural width, and SL=standard length.

1DPH	EPL	EPA	PHPL	PHPA	HYPL	HYPW	SL
EPL	**0.05 (0.02,0.08)** *0.48 (0.21,0.76)*	0.28 (-0.20,0.81)	0.97 (0.93,1.00)*	-0.59 (-1.00,-0.16)*	0.66 (0.39,0.91)*	0.78 (0.58,0.96)*	0.55 (0.18,0.83)*
EPA	0.07 (-0.04,0.19)	**0.18 (0.05,0.31)** *0.13 (0.04,0.22)*	0.35 (-0.15,0.81)	-0.47 (-0.95,0.08)	0.52 (0.10,0.93)*	0.44 (-0.02,0.87)	0.47 (0,0.87)*
PHPL	0.42 (0.18,0.67)	0.08 (-0.03,0.19)	**0.05 (0.02,0.08)** *0.40 (0.16,0.62)*	-0.52 (-0.90,-0.02)*	0.72 (0.49,0.94)*	0.75 (0.52,0.94)*	0.52 (0.15,0.83)*
PHPA	-0.13 (-0.25,-0.02)	-0.05 (-0.12,0.01)	-0.10 (-0.21,0)	**0.18 (0.04,0.31)** *0.10 (0.02,0.18)*	-0.72 (-1.0,-0.33)*	-0.77 (-1.0,-0.46)*	-0.82 (-1.10,-0.53)*
HYPL	0.41 (0.12,0.71)	0.17 (0.01,0.33)	0.41 (0.13,0.69)	-0.21 (-0.37,-0.05)	**0.04 (0.02,0.06)** *0.81 (0.36,1.28)*	0.8 (0.61,0.95)*	0.87 (0.73,0.97)*
HYPW	0.47 (0.15,0.77)	0.14 (-0.02,0.28)	0.42 (0.14,0.69)	-0.21 (-0.37,-0.06)	0.63 (0.24,1.04)	**0.02 (0.01,0.04)** *0.76 (0.34,1.19)*	0.83 (0.66,0.95)*
SL	0.36 (0.07,0.66)	0.16 (-0.01,0.32)	0.31 (0.03,0.56)	-0.24 (-0.42,-0.07)	0.73 (0.27,1.17)	0.68 (0.28,1.13)	**0.01 (0.01, 0.02)** *0.88 (0.35,1.35)*

15DPH	EPL	EPA	PHPL	PHPA	HYPL	HYPW	SL
EPL	**0.11 (0.05,0.18)** *0.73 (0.36,1.12)*	-0.02 (-0.64,0.57)	0.97 (0.95,1)*	0.21 (-0.26,0.64)	0.69 (0.42,0.89)*	0.83 (0.68,0.96)*	0.67 (0.41,0.88)*
EPA	0 (-0.14,0.12)	**0.06 (0.01, 0.12)** *0.1 (0.01,0.19)*	0.07 (-0.53,0.67)	0.28 (-0.35,1.04)	-0.06 (-0.65,0.58)	-0.04 (-0.63,0.6)	0.03 (-0.55,0.67)
PHPL	0.72 (0.33,1.07)	0.02 (-0.12,0.14)	**0.11 (0.05, 0.16)** *0.75 (0.36,1.14)*	0.29 (-0.16,0.7)	0.65 (0.38,0.89)*	0.78 (0.59,0.93)*	0.56 (0.25,0.82)*
PHPA	0.09 (-0.08,0.26)	0.04 (-0.04,0.12)	0.12 (-0.06,0.29)	**0.16 (0.07, 0.27)** *0.24 (0.09,0.39)*	0.14 (-0.31,0.63)	0.2 (-0.23,0.68)	-0.1 (-0.56,0.37)
HYPL	0.4 (0.13,0.68)	-0.01 (-0.12,0.09)	0.38 (0.11,0.65)	0.05 (-0.09,0.19)	**0.04 (0.02, 0.07)** *0.46 (0.2,0.72)*	0.87 (0.74,0.97)*	0.85 (0.70,0.95)*
HYPW	0.54 (0.22,0.85)	-0.01 (-0.13,0.10)	0.52 (0.2,0.82)	0.07 (-0.08,0.22)	0.45 (0.18,0.72)	**0.04 (0.02, 0.06)** *0.58 (0.26,0.89)*	0.87 (0.75,0.96)*
SL	0.44 (0.15,0.74)	0.01 (-0.11,0.12)	0.37 (0.1,0.66)	-0.04 (-0.19,0.12)	0.44 (0.19,0.72)	0.51 (0.2,0.79)	**0.04 (0.02, 0.06)** *0.58 (0.28,0.9)*

100DPH	EPL	EPA	PHPL	PHPA	HYPL	HYPW	SL
EPL	**0.30 (0.14, 0.45)** *0.66 (0.29,0.98)*	-0.17 (-0.64,0.35)	0.93 (0.87,0.99)*	0.16 (-0.37,0.72)	0.61 (0.3,0.84)*	0.81 (0.65,0.96)*	0.52 (0.21,0.82)*
EPA	-0.05 (-0.19,0.08)	**0.09 (0.03, 0.16)** *0.15 (0.05,0.26)*	-0.07 (-0.58,0.42)	-0.51 (-1.01,0.06)	0.10 (-0.44,0.62)	0.01 (-0.49,0.55)	0.11 (-0.42,0.61)
PHPL	0.63 (0.29,0.96)	-0.02 (-0.1,0.12)	**0.3 (0.15, 0.4)** *0.69 (0.32,1.05)*	0.33 (-0.17,0.84)	0.55 (0.23,0.83)*	0.78 (0.58,0.93)*	0.43 (0.08,0.76)*
PHPA	0.04 (-0.08,0.18)	-0.07 (-0.1,0.01)	0.09 (-0.04,0.24)	**0.01 (-0.03, 0.05)** *0.12 (0.02,0.21)*	0.10 (-0.47,0.65)	0.31 (-0.25,0.78)	-0.03 (-0.57,0.54)
HYPL	0.35 (0.1,0.6)	0.03 (-0.1,0.14)	0.32 (0.08,0.58)	0.02 (-0.10,0.13)	**0.13 (0.05, 0.21)** *0.5 (0.21,0.76)*	0.82 (0.65,0.95)*	0.91 (0.81,0.98)*
HYPW	0.54 (0.22,0.84)	0 (-0.12,0.15)	0.53 (0.21,0.85)	0.09 (-0.04,0.22)	0.47 (0.18,0.75)	**0.20 (0.09, 0.3)** *0.66 (0.31,1.03)*	0.73 (0.50,0.91)*
SL	0.33 (0.05,0.58)	0.03 (-0.10,0.17)	0.28 (0.01,0.53)	-0.01 (-0.13,0.12)	0.50 (0.19,0.76)	0.46 (0.15,0.74)	**0.09 (0.05, 0.14)** *0.6 (0.28,0.94)*

Table S8: Estimated differences (with approximate 95% CI in parentheses) between each pair of ages in genetic variances (bold font, diagonal), heritabilities (italic font, diagonal) and correlations (above diagonal). For each of these differences, the second age was subtracted from the first so a negative value reflects a higher value in an older age relative to a younger age. Asterisks denote significant differences in age specific parameters as evidenced by confidence intervals that do not span zero. EPL=Epural length, EPA=Epural angle, PHPL=parahypural length, PHPA=parahypural angle, HYPL=hypural length, HYPW=hypural width, and SL=standard length.

1 vs 15 DPH	EPL	EPA	PHPL	PHPA	HYPL	HYPW	SL
EPL	**-0.06 (-0.13, 0.001)** *-0.25 (-0.71, 0.22)*	0.30 (-0.46,1.1)	-0.004 (-0.05,0.04)	-0.80 (-1.38,-0.14)*	-0.02 (-0.37,0.39)	-0.05 (-0.31,0.2)	-0.12 (-0.52,0.33)
EPA		**0.11 (-0.01, 0.26)** *0.04 (-0.09, 0.16)*	0.28 (-0.52,1.05)	-0.75 (-1.69,0.14)	0.58 (-0.15,1.34)	0.48 (-0.26,1.28)	0.45 (-0.3,1.22)
PHPL			**-0.05 (-0.12,0.01)** *-0.35 (-0.82, 0.09)*	-0.80 (-1.39,-0.11)*	0.08 (-0.29,0.45)	-0.03 (-0.31,0.26)	-0.04 (-0.52,0.42)
PHPA				**0.02 (-0.16,0.18)** *-0.14 (-0.31, 0.04)*	-0.86 (-1.45,-0.25)*	-0.97 (-1.53,-0.42)*	-0.72 (-1.28,-0.18)*
HYPL					**-0.01 (-0.04,0.03)** *0.35 (-0.18, 0.91)*	-0.07 (-0.3,0.15)	0.02 (-0.17,0.22)
HYPW						**-0.01 (-0.04,0.01)** *0.18 (-0.25, 0.7)*	-0.04 (-0.24,0.15)
SL							**-0.02 (-0.04, -0.002)*** *0.29 (-0.3, 0.85)*

1 vs 100 DPH	EPL	EPA	PHPL	PHPA	HYPL	HYPW	SL
EPL	**-0.25 (-0.41, -0.09)*** *-0.17 (-0.64, 0.23)*	0.45 (-0.26,1.08)	0.04 (-0.04,0.11)	-0.7 (-1.46,-0.09)*	0.05 (-0.36,0.45)	-0.03 (-0.29,0.23)	0.03 (-0.41,0.49)
EPA		**0.09 (-0.05, 0.23)** *-0.02 (-0.16, 0.12)*	0.42 (-0.25,1.09)	0.03 (-0.71,0.82)	0.43 (-0.21,1.13)	0.43 (-0.25,1.1)	0.36 (-0.25,1.04)
PHPL			**-0.24 (-0.41, -0.09)*** *-0.29 (-0.71, 0.15)*	-0.85 (-1.59,-0.19)*	0.17 (-0.24,0.58)	-0.02 (-0.33,0.26)	0.09 (-0.44,0.55)
PHPA				**0.11 (-0.03, 0.26)** *-0.02 (-0.13, 0.12)*	-0.82 (-1.57,-0.19)*	-1.08 (-1.68,-0.45)*	-0.79 (-1.45,-0.15)*
HYPL					**-0.1 (-0.17, -0.02)*** *0.31 (-0.27, 0.84)*	-0.02 (-0.27,0.24)	-0.04 (-0.21,0.1)
HYPW						**-0.18 (-0.29, -0.07)*** *0.1 (-0.44, 0.66)*	0.11 (-0.15,0.38)
SL							**-0.08 (-0.13, -0.03)*** *0.27 (-0.37, 0.83)*

15 vs 100 DPH	EPL	EPA	PHPL	PHPA	HYPL	HYPW	SL
EPL	**-0.19 (-0.36, -0.02)*** *0.07(-0.44, 0.59)*	0.15 (-0.63,0.92)	0.04 (-0.02,0.12)	0.05 (-0.64,0.8)	0.07 (-0.34,0.43)	0.02 (-0.21,0.23)	0.14 (-0.26,0.56)
EPA		**-0.03 (-0.12, 0.06)** *-0.06(-0.19, 0.08)*	0.14 (-0.63,0.99)	0.79 (-0.14,1.71)	-0.15 (-0.97,0.66)	-0.05 (-0.86,0.8)	-0.08 (-0.84,0.76)
PHPL			**-0.19 (-0.36, -0.04)*** *0.06 (-0.51, 0.57)*	-0.04 (-0.76,0.62)	0.1 (-0.31,0.52)	0 (-0.25,0.26)	0.13 (-0.33,0.61)
PHPA				**0.1 (-0.01, 0.21)** *0.12 (-0.06, 0.3)*	0.04 (-0.7,0.77)	-0.12 (-0.83,0.57)	-0.07 (-0.86,0.63)
HYPL					**-0.09 (-0.16, -0.01)*** *-0.03 (-0.42, 0.34)*	0.05 (-0.13,0.29)	-0.06 (-0.23,0.1)
HYPW						**-0.2 (-0.27, -0.05)*** *-0.08 (-0.55, 0.4)*	0.15 (-0.06,0.42)
SL							**-0.06 (-0.11, -0.004)*** *-0.02 (-0.45, 0.45)*

Table S9: Test of Cheverud's conjecture that **P** can be used as a surrogate for **G**. Confidence intervals based on Estimated differences (with 95% CI in parentheses) between phenotypic and genetic correlations at 1, 15, and 100 DPH are depicted on the off-diagonals. Significant differences are noted when 95% CI do not span zero. EPL=Epural length, EPA=Epural angle, PHPL=parahypural length, PHPA=parahypural angle, HYPL=hypural length, HYPW=hypural width, and SL=standard length.

1 DPH	EPL	EPA	PHPL	PHPA	HYPL	HYPW	SL
EPL		-0.25 (-0.73,0.25)	-0.11 (-0.15,-0.06)*	0.39 (-0.04,0.81)	-0.17 (-0.44,0.11)	-0.21 (-0.4,0)	-0.11 (-0.43,0.23)
EPA			-0.30 (-0.79,0.19)	-0.10 (-0.65,0.35)	-0.37 (-0.79,0.05)	-0.28 (-0.70,0.17)	-0.30 (-0.76,0.13)
PHPL				0.41 (-0.06,0.85)	-0.19 (-0.40,0.09)	-0.19 (-0.39,0.05)	-0.11 (-0.42,0.26)
PHPA					0.43 (0.05,0.79)*	0.45 (0.11,0.77)*	0.53 (0.23,0.83)*
HYPL						-0.12 (-0.28,0.08)	-0.14 (-0.25,0.01)
HYPW							-0.10 (-0.25,0.06)
SL							

15 DPH	EPL	EPA	PHPL	PHPA	HYPL	HYPW	SL
EPL		-0.05 (-0.66,0.55)	-0.09 (-0.13,-0.06)*	-0.14 (-0.6,0.32)	-0.12 (-0.36,0.13)	-0.14 (-0.29,0.02)	-0.08 (-0.3,0.20)
EPA			-0.11 (-0.73,0.47)	-0.71 (-1.55,-0.11)*	-0.004 (-0.67,0.62)	-0.01 (-0.64,0.61)	-0.04 (-0.7,0.58)
PHPL				-0.16 (-0.60,0.29)	-0.08 (-0.32,0.21)	-0.11 (-0.28,0.09)	-0.004 (-0.27,0.32)
PHPA					-0.14 (-0.63,0.35)	-0.11 (-0.53,0.39)	0.04 (-0.42,0.51)
HYPL						-0.11 (-0.22,0.03)	-0.04 (-0.16,0.10)
HYPW							-0.004 (-0.1,0.11)
SL							

100 DPH	EPL	EPA	PHPL	PHPA	HYPL	HYPW	SL
EPL		0.04 (-0.47,0.55)	-0.14 (-0.22,-0.07)*	-0.13 (-0.69,0.42)	-0.17 (-0.44,0.14)	-0.22 (-0.38,-0.03)	-0.13 (-0.43,0.21)
EPA			0.02 (-0.49,0.55)	0.23 (-0.37,0.75)	-0.11 (-0.62,0.42)	0.004 (-0.52,0.52)	-0.08 (-0.6,0.42)
PHPL				-0.22 (-0.72,0.33)	-0.17 (-0.49,0.16)	-0.2 (-0.37,0.002)	-0.12 (-0.45,0.25)
PHPA					-0.08 (-0.66,0.53)	-0.2 (-0.71,0.37)	0.01 (-0.53,0.64)
HYPL						-0.09 (-0.24,0.08)	-0.14 (-0.23,-0.04)*
HYPW							-0.01 (-0.19,0.22)
SL							

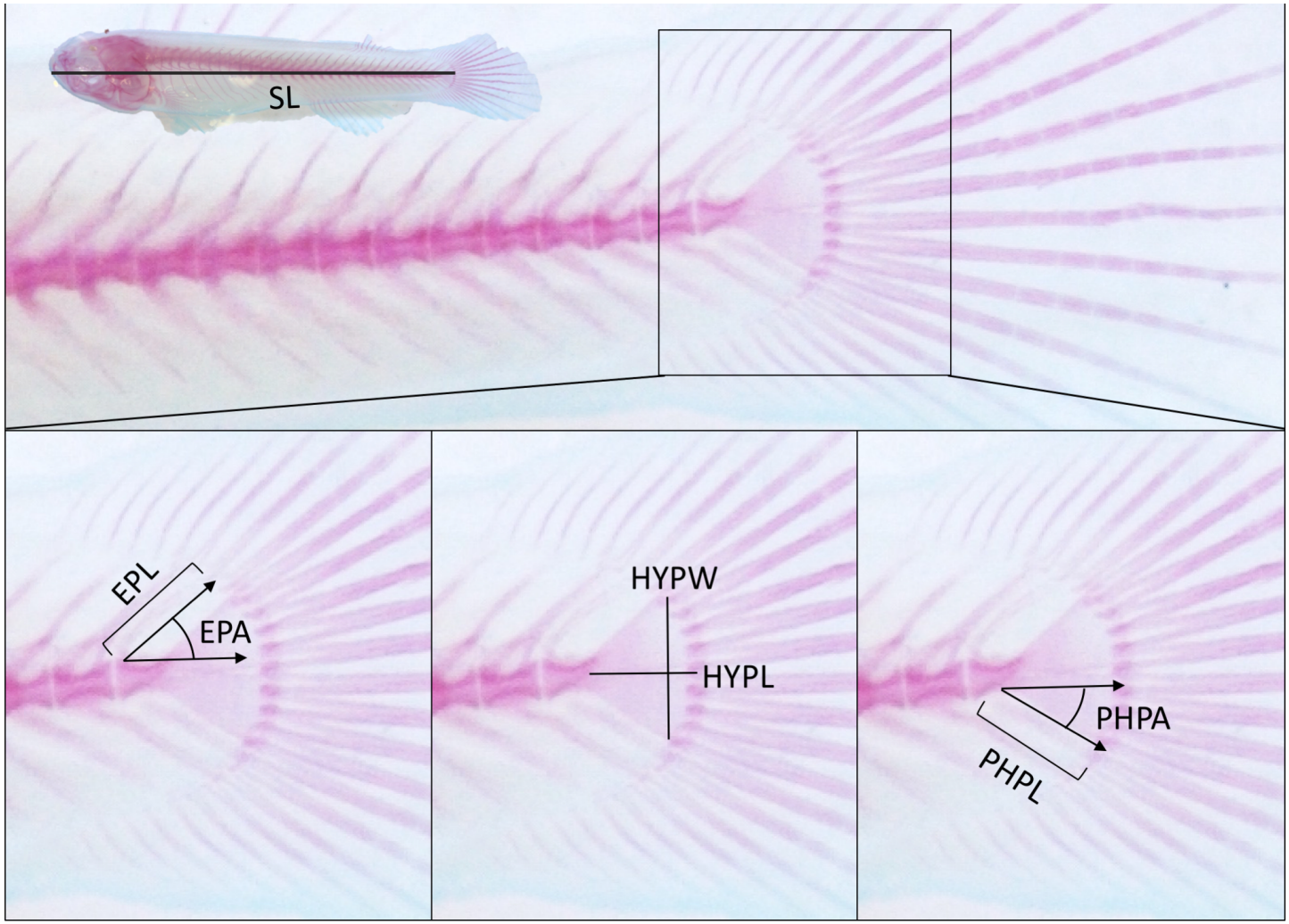

Figure S1: Cleared and stained *K. marmoratus* specimen. EPA=epural angle, EPL=epural length, HYPL=length of the hypurals, HYPW=width of the hypurals, PHPA=parahypural angle, PHPL=parahypural length, and SL=standard length measurements are shown.

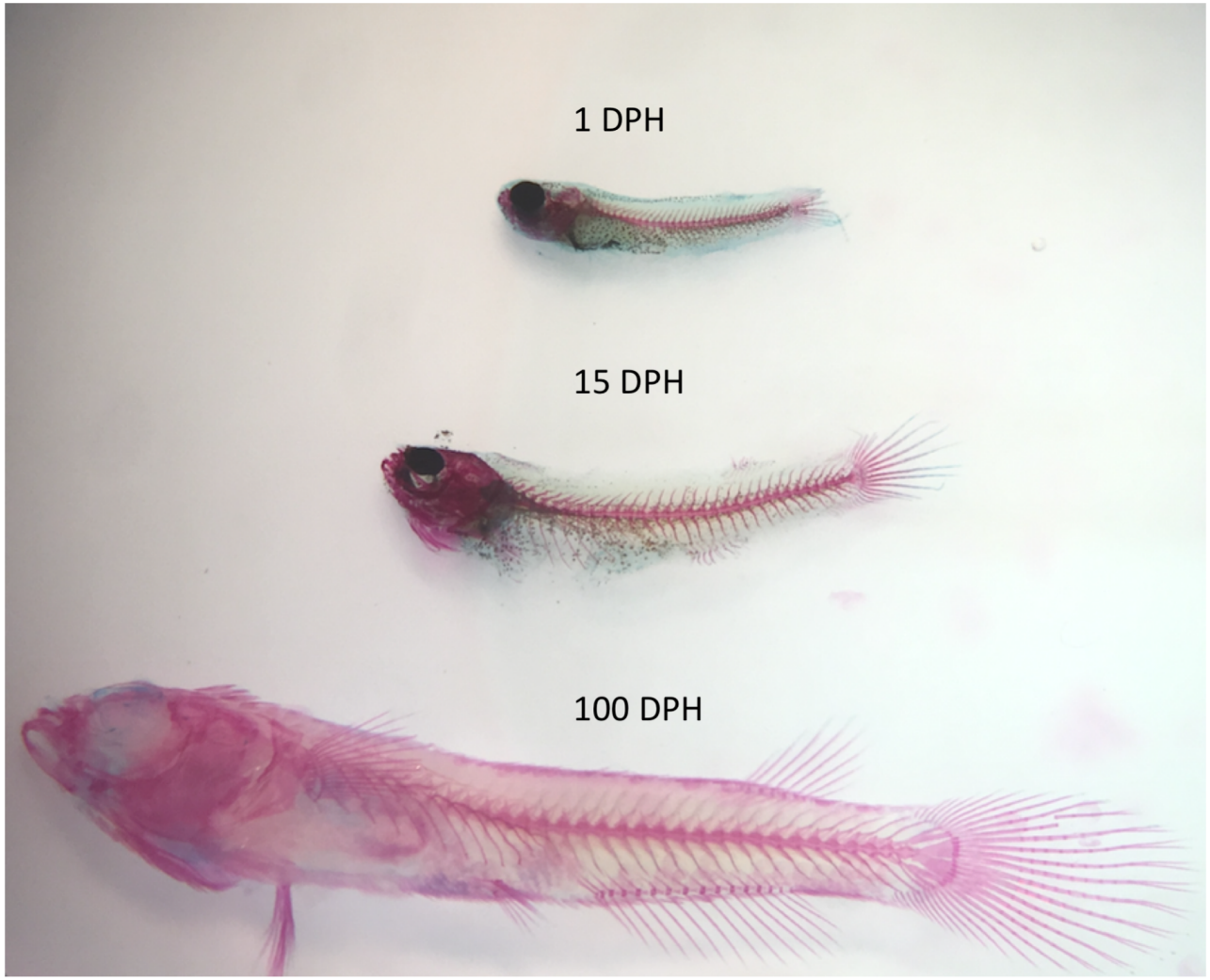

Figure S2: Typical cleared and stained specimen at each age (Top to bottom: 1, 15, and 100 DPH).